Sensorineural Hearing Loss in Otosclerosis Surgery

Kristýna Néma[1,2,3,*], Viktor Chrobok[2,3], Jan Mejzlík[2,3], Vladimír Pavlík[1], Lukáš Školoudík[2,3]

ABSTRACT

Background: During otosclerosis surgery, operative trauma can lead to decreased bone conduction.
Aims: The study aims to observe the bone conduction changes after otosclerosis operations and analyse possible factors affecting the postoperative decrease in bone conduction.
Material and Methods: Authors retrospectively processed the data of 109 patients and evaluated pure tone audiometry before surgery and consequently 2 days, 1 month and 1 year after surgery.
Results: We noted a deterioration of bone conduction >5 dB on the second postoperative day in 28% (30/109) of patients, which persisted one year after the surgery in 9% (10/109) cases. Analysis of individual factors affecting bone conduction loss revealed a higher risk of permanent loss of bone conduction in patients with early postoperative loss in higher frequencies, in older patients and patients with a preoperative threshold of bone conduction >20 dB. Revision surgery was not a statistically significant factor.
Conclusion and Significance: The bone conduction decrease after otosclerosis surgery is usually temporary. The recovery of bone conduction is influenced by the age of patients and the level of bone conduction before the surgery. The early postoperative decrease of bone conduction in higher frequencies is a negative predictive factor for permanent hearing loss.

KEYWORDS

otosclerosis; surgical trauma; sensorineural hearing loss

AUTHOR AFFILIATIONS

[1] Department of Military Internal Medicine and Military Hygiene, Military Faculty of Medicine, University of Defence, Czech Republic
[2] Department of Otorhinolaryngology and Head and Neck Surgery, University Hospital Hradec Králové, Czech Republic
[3] Faculty of Medicine in Hradec Králové, Charles University, Czech Republic
* Corresponding author: Department of Otorhinolaryngology and Head and Neck Surgery University, Hospital Hradec Králové, Sokolská 581, 500 05 Hradec Králové, Czech Republic; kristyna.nema@fnhk.cz

Received: 29 November 2024
Accepted: 17 December 2024
Published online: 18 February 2025

Acta Medica (Hradec Králové) 2024; 67(3): 73–78
https://doi.org/10.14712/18059694.2025.1

INTRODUCTION

Otosclerosis is a disease of the inner ear bony labyrinth. The most frequent symptoms are hearing loss, conductive or mixed, and tinnitus (1). The cause of conductive hearing loss is the fixation of the stapes to the oval window. The cause of the sensorineural hearing loss is not fully explained (2–4).

The causal treatment of otosclerosis is currently unknown. Thus, the surgical effort focuses on the disease's main symptom, conductive hearing loss. The surgery is considered if the air-bone gap is greater than 20 dB (5). The replacement of stapes with prostheses is the basic principle of the operation. The surgical techniques have improved a lot in the last decades; however, the basic principle of the operation has not changed since the 1950s.

This article aims to analyse the audiological outcomes of otosclerosis surgery for 1 year, to monitor the change of bone conduction in pure tone audiometry after the surgery and to find predictive factors indicating permanent hearing loss due to surgical trauma.

MATERIAL AND METHODS

The retrospective study evaluated data from patients diagnosed with otosclerosis who were operated on at the Department of Otorhinolaryngology and Head and Neck Surgery in the period 2013–2017.

In the case of primary operation, the predominant method was stapedotomy with piston (titanium) insertion, which was performed in 88 (81%) patients. The complete stapedectomy with removing the entire stapedial footplate was performed in only 1 (1%) case.

During the revision operations, a manubrio-vestibulopexy was performed in 3 (3%) patients. In 6 (6%) patients, the adhesions were disrupted, and the original prosthesis was left; in 11 (10%) patients, the original prosthesis was replaced with a new one.

In our workplace, we use cold instruments as standard for platinotomy – a perforator and hooks on the stapes footplate. Neither a power drill nor a laser were used for platinotomy. We follow the rule of not suctioning directly from the hole of the oval window after perforation of the footplate. In our group, it was impossible to retrospectively determine the suction data and use it for statistical analysis due to the insufficient description of this procedure in the operative protocol.

The pure tone audiograms were recorded for each patient before surgery, 2 days (only bone conduction), 1 month, and 1 year after surgery. For the statistical analysis, we evaluated four crucial frequencies (0.5, 1, 2, 4 kHz) of bone conduction before surgery, 2 days, 1 month and 1 year after surgery, air conduction before surgery, 1 month and 1 year after surgery. Possible predictive factors leading to permanent hearing damage due to surgical trauma were analysed (6, 7). These were:

1. Age – younger than 40 years and aged 40 and older
2. Gender – men and women
3. Type of surgery – first surgery and revision surgery
4. Preoperative sensorineural component of hearing loss – £20 dB and >20 dB
5. Side of the surgery – left and right ear

We considered an impairment of >5 dB as a significant bone conduction impairment. The following tests were used for statistical processing: the Kolmogorov-Smirnov, Spearman and Fisher exact tests.

RESULTS

In the study period, 143 patients were operated for otosclerosis. After excluding patients with incomplete documentation, 109 patients were analysed: 78 (72%) women and 31 (28%) men. Primary surgery was performed in 89 (82%) cases and revision in 20 (18%) cases. The right ear was operated in 51 (47%) cases and the left ear in 58 (53%) cases. The average age was 47 (±11) years. There were 84 (77%) patients aged 40 years and older and 25 (23%) younger than 40 years.

Before the surgery, the average hearing loss at the observed frequencies was 56 (±15) dB, and the bone-air gap was 30 (±9) dB.

One month after the surgery, hearing improved by an average of 19 (±18) dB, hearing improved in 101 (93%) patients, and a significant improvement of >10 dB occurred in 82 (75%) patients (Figure 1). The average bone-air gap was 12 (±8) dB, bone-air gap £ 10 dB was in 59 (54%) patients.

One year after the surgery, the average hearing improvement was 23 dB (±16), hearing improved in 102 (94%) patients, and significant improvement >10 dB in 91 (84%) patients. The average bone-air gap was 10 (±8) dB, bone-air gap £10 dB was in 69 (63%) patients.

During revision surgeries, hearing improved in all 20 (100%) patients 1 month after surgery. The average bone conduction value of the patients before surgery was 26 (±16) dB. On the second postoperative day, the average bone conduction value was 29 (±12) dB. Worsening occurred in 30 (28%) patients. The difference was statistically significant (p = 0.020). One year after surgery, the average value of bone conduction was 23 (±11) dB; compared to the preoperative state, deterioration was noted in 10 (9%) patients, but the decrease was not statistically significant (p = 0.12) (Figure 2). There were no major postoperative complications, and deafening of the operated ear did not occur in any patient.

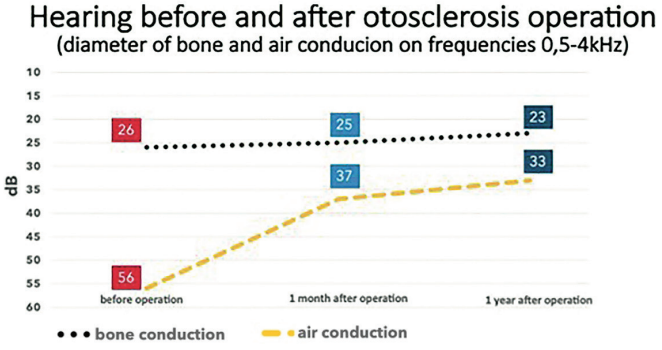

Fig. 1 Hearing before and after stapes surgery (diameter of bone and air conduction on frequencies 0,5–4 kHz).

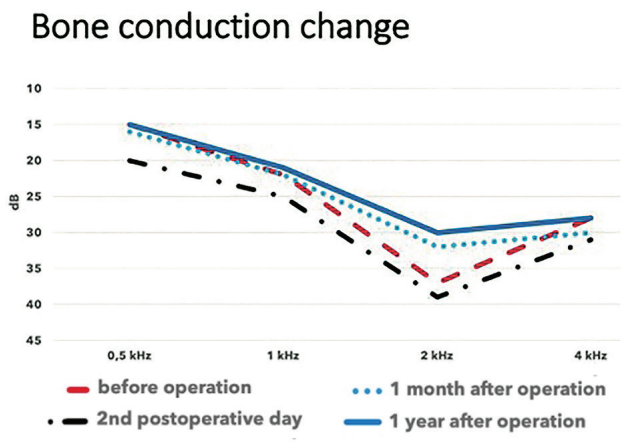

Fig. 2 Bone conduction – before surgery, second postoperative day, 1 month and 1 year after surgery.

frequency	2nd postoperative day age < 40 (n = 25)	1 year after operation age < 40 (n = 25)	2nd postoperative day age ≥ 40 (n = 84)	1 year after operation age ≥ 40 (n = 84)
0,5 kHz	5 (20%)	2 (8%)	25 (30%)	7 (8%)
1 kHz	4 (16%)	2 (8%)	21 (25%)	9 (11%)
2 kHz	6 (24%)	3 (12%)	20 (24%)	6 (7%)
4 kHz	4 (16%)	3 (12%)	21 (25%)	***17 (20%) p = 0,01***

Tab. 1 Number of patients with a decrease in bone conduction (≥10 dB) in relation to age.

When analysing the average bone conduction changes at individual frequencies on the second postoperative day, the decreases were greater in lower frequencies. One year after surgery, bone conduction improved at a frequency of 2 kHz compared to the preoperative audiogram. At other frequencies, the average value of bone conduction corresponded to the preoperative status (Figure 2). Patients who had early postoperative bone conduction loss ≥ 10 dB at frequencies of 2 and 4 kHz remained significantly impaired bone conduction one year after surgery ($p<0.025$).

EFFECT OF AGE ON POSTOPERATIVE DECREASE IN BONE CONDUCTION

We compared the postoperative decrease in bone conduction in patients aged 40 years and older (84 patients – 77%) and patients younger than 40 years (25 patients – 23%). In elderly patients, the preoperative mean bone conduction value was 27 (±11) dB. On the second postoperative day, the average bone conduction value was 31 (±11) dB; deterioration occurred in 25 out of 84 (30%) operated patients, and the decrease was statistically significant ($p = 0.048$).

One year after surgery, the average value of bone conduction was 25 (±12) dB. We noted a deterioration compared to the preoperative condition in only 8 (10%) patients; the decrease was not statistically significant ($p>0.1$).

In patients younger than 40, the preoperative mean value of bone conduction was 19 (±5) dB. On the second postoperative day, the average bone conduction value was 23 (±12) dB, and deterioration occurred in 4 out of 25 (16%) patients. The difference was not statistically significant ($p = 0.073$). One year after surgery, the average value of bone conduction was 18 (±8) dB. We noted a deterioration compared to the preoperative condition in only 2 (8%) patients; the decrease was not statistically significant ($p>0.1$). When analysing individual frequencies, on the second postoperative day, there was a statistically significant decrease in bone conduction in patients aged 40 and older at all frequencies compared to patients younger than 40 ($p<0.025$). One year after surgery, we noted a significant difference between the groups of younger and older patients only at a frequency of 4 kHz ($p = 0.010$) (Table 1).

THE INFLUENCE OF THE PREOPERATIVE SENSORINEURAL COMPONENT OF HEARING LOSS ON THE POSTOPERATIVE DECREASE IN BONE CONDUCTION

Preoperatively, 43 (39%) patients had a normal mean bone conduction value (£20 dB). In this group, deterioration of bone conduction occurred on the second postoperative day in 15 (35%) patients, and deterioration persisted in 3 (7%) patients one year after surgery ($p = 0.25$). In the group of 66 (61%) patients with a preoperatively bone conduction threshold >20 dB, deterioration of bone conduction occurred on the second postoperative day in 15 (23%) patients. The deterioration persisted in 7 (11%) patients a year after surgery. When analysing individual frequencies, we demonstrated a statistically significantly greater decrease in bone conduction at 1 and 4 kHz on the second postoperative day and one year after surgery in patients with a preoperative sensorineural component of hearing loss >20 dB

frequency	2nd postoperative day BC ≤ 20 dB (n = 43)	1 year after operation BC ≤ 20 dB (n = 43)	2nd postoperative day BC > 20 dB (n = 66)	1 year after operation BC > 20 dB (n = 66)
0,5 kHz	15 dB	10 dB	24 dB	18 dB
1 kHz	18 dB	14 dB	30 dB	***25 dB*** ***p = 0,001***
2 kHz	32 dB	22 dB	44 dB	35 dB
4 kHz	21 dB	16 dB	38 dB	***36*** dB ***p = 0,001***

Tab. 2 Number of patients with a decrease in bone conduction (≥10 dB) in relation to preoperative bone conduction threshold.

(p<0.001), the differences were not significant at the 2 kHz frequency (p>0.1), at the deep frequency of 0.5 kHz, on the other hand, there was a significantly greater decrease in patients with preoperatively normal bone conduction (p<0.001) (Table 2).

IMPACT OF REVISION OPERATION

During revision operations, the sensorineural component worsened in 4 (20%) out of 20 patients; bone conduction was adjusted to the preoperative level in all patients within a year of the operation. Compared with primary operations, no statistically significant difference in bone conduction decrease was noted (p>0.1).

DISCUSSION

Sensorineural hearing loss in patients with otosclerosis develops as part of the disease itself. So far, it has not been clarified precisely how the auditory epithelium of the inner ear is affected. Current studies show a relationship between the inflammatory involvement of the inner ear by the measles virus and cytokines released from otosclerotic foci (8). During the histological examination of an otosclerotic deposit, we can find different cellular activity, according to which otosclerotic deposits are divided into four stages. The cellularity of the deposit, the presence of osteoclasts and osteoblasts, vascularisation and the amount of intercellular collagen matrix are evaluated. Stage I indicates the most active deposits, and stage IV is completely inactive deposits (8). In the early stages, cytokines TNF-α, interleukin-1, interleukin-6, parts of the complement C3a, C3b, and C5a are released from the otosclerotic deposit. These molecules penetrate the perilymph and can affect the function of the hair cells of the inner ear (9–11). The greatest attention is paid to the cytokine TNF-α, which increases the activity of osteoclasts and, thus, pathological bone remodelling (2, 3).

The development of radiodiagnostic techniques enables targeted imaging of the area of otosclerotic deposits. Shin et al. demonstrate on HRCT a relationship between the extent of the otosclerotic deposit of the otic capsule and the degree of sensorineural hearing loss. In patients with HRCT, evidence of an otosclerotic deposit spreading into the endosteum showed a significant decrease in bone conduction (12).

In patients undergoing surgery for otosclerosis, there is a new factor contributing to the deterioration of the sensorineural component of hearing loss – surgical trauma. This risk leads operators to introduce new modifications of the original operation – stapedectomy. Today, it is already standard practice to switch to operations preserving a larger part of the stapes plate with an effort to create an opening corresponding to the size of the stapes prosthesis. This significantly reduces perilymph leakage during surgery and in the early postoperative period and reduces the risk of worsening sensorineural hearing loss (13–15).

In our group of patients, the stapedotomy technique completely prevailed. Removal of the entire footplate (stapedectomy) was performed in only one patient.

The risk of postoperative hearing loss is not the same at all hearing frequencies. Several works deal with the frequency-specific analysis of postoperative deterioration of bone conduction (16, 17). Losses are more often noted in higher frequencies. Strömbäck et al. reported deterioration of bone conduction at frequencies 4–8 kHz >10 dB in 6.5% of patients (17).

In our group of patients, the early decrease in bone conduction was greater in lower frequencies, but the early decrease in high frequencies is more prognostically significant. In patients who experienced a decrease in bone conduction at frequencies of 2 and 4 kHz on the second postoperative day, significantly worse bone conduction persisted even one year after surgery. We observed an overall postoperative improvement in bone conduction at a frequency of 2 kHz. It could be explained by a Carhart notch theory (24). Carhart attributed the phenomenon of a reduction in bone conduction sensitivity with the peak in 2 kHz to "mechanical factors associated with stapedial fixation." The Carhart notch is not an accurate indication of "cochlear reserve", and this apparent bone conduction loss may be corrected by surgical intervention (25, 26).

One of the possible risk factors for postoperative decrease in bone conduction is pre-existing sensorineural hearing loss. Currently, this risk factor is not clearly accepted. Most studies demonstrate a higher risk of postoperative hearing impairment in patients with preoperative sensorineural hearing loss (16–20); however, studies refuting this have also been published (16). In our set, the results were also ambiguous, the decrease varied at individual frequencies. We noted a more significant decrease

in preoperative sensorineural hearing loss at frequencies of 1 and 4 kHz; at a frequency of 2 kHz, the difference was not significant, and at a deep frequency of 0.5 kHz, on the contrary, the decrease was lower compared to the normal preoperative bone conduction threshold.

The risk of traumatising the structures of the inner ear comes at the stage of handling the stapes plate. Yin et al. did not demonstrate acoustic trauma in cadavers when milling the footplate with a diamond bur but did demonstrate the risk of acoustic trauma from suction noise in the oval window fossa (20).

Attention is also paid to the age of the patients. Bauchet et al. in their analysis, demonstrated a higher sensitivity to early (4–6 weeks after surgery) postoperative deterioration of bone conduction in patients older than 40 years (16). However, when checked 9 months after the operation, the difference against younger patients was no longer statistically significant, and the authors do not consider age to be a risk factor for permanent hearing impairment due to surgical trauma. In our group of patients, the early decrease in bone conduction was significantly greater in older patients at all frequencies, one year after surgery only at the frequency of 4 kHz ($p = 0.010$). A frequently discussed issue is revision operations. Otosclerosis reoperations are considered risky for inner ear damage, the results of revision operations are uncertain (21–23). In our file, the revision operations that were performed were successful. One month after the operation, all patients experienced improved hearing. One year post-operation, 95% of patients showed an average improvement of more than 10 dB. The results also demonstrated that, compared to primary operations, our group did not exhibit a higher risk of bone conduction decline.

LIMITATIONS

This study has several limitations. First, it is a retrospective study, which inherently carries risks of bias and incomplete data. Additionally, incomplete documentation posed challenges in analysing all relevant variables. Some patients missed their scheduled follow-up appointments, while others attended follow-ups at different healthcare facilities, making it difficult to track their outcomes. Finally, certain medical records were unavailable or could not be retrieved, further limiting the completeness of the data.

CONCLUSION

Stapes surgeries improve air conduction in more than 90% of patients. However, surgical trauma could decrease bone conduction. In most patients, the decrease of bone conduction after surgery is only temporary. There is a higher risk of permanent sensorineural loss in patients with a postoperative decrease in bone conduction in higher frequencies (2 and 4 kHz) 2 days after the surgery, in patients aged 40 years and more (for frequency 4 kHz) and in patients with a pre-existing sensorineural component of hearing loss (for frequencies 1 and 4 kHz).

ETHICAL APPROVAL

The study was conducted retrospectively using fully anonymised data, which means that no personal or identifiable information about patients was accessed or used. As a result, the study did not involve any interventions or direct contact with patients, and there was no risk to their privacy or well-being. For these reasons, approval from the ethics committee was not required.

DISCLOSURE STATEMENT

No potential conflict of interest was reported by the author(s).

FUNDING

This work was supported by the scientific program of Charles University, Faculty of Medicine in Hradec Kralove Cooperatio Program, research area SURG.

REFERENCES

1. Ealy M, Smith R.J.H. Otosclerosis. Online. In: ALFORD, R.L. a SUTTON, V.R. (ed.). *Medical Genetics in the Clinical Practice of ORL*. Advances in Oto-Rhino-Laryngology. S. Karger, 2011: 122–129.
2. Karosi T, Jókay I, Kónya J, et al. Detection of osteoprotegerin and TNF-alpha mRNA in ankylotic stapes footplates in connection with measles virus positivity. Laryngoscope. 2006 Aug; 116(8): 1427–33.
3. Zou J, Pyykkö I, Sutinen P, et al. Vibration induced hearing loss in guinea pig cochlea: expression of TNF-alpha and VEGF. Hear Res. 2005 Apr; 202(1–2): 13–20.
4. Sziklai I, Batta TJ, Karosi T. Otosclerosis: an organ-specific inflammatory disease with sensorineural hearing loss. Eur Arch Otorhinolaryngol. 2009 Nov; 266(11): 1711–1718.
5. Alberti A, Figuerola E, Romero-Farina G, et al. Otosclerosis and Preoperative Small Air-Bone Gap. Audiol Neurotol. 2017; 22: 350–355.
6. Bauchet St. Martin, Michele, Rubinstein, Elaine N, Hirsch, Barry E. High-Frequency Sensorineural Hearing Loss After Stapedectomy. Otol Neurotol. 2008 Jun; 29(4): 447–52.
7. Sobrinho PG, Oliveira CA, Venosa AR. Long-Term Follow-Up of Tinnitus in Patients with Otosclerosis After Stapes Surgery. Int Tinnitus J. 2004; 10(2): 197–201.
8. Iyer V, Gristwood RE. Histopathology of the stapes in otosclerosis. Pathology. 1984 Jan; 16(1): 30–38.
9. Sziklai I. Human otosclerotic bone-derived peptide decreases the gain of the electromotility in isolated outer hair cells. Hear Res. 1996 May; 95(1–2): 100–7.
10. Fujioka M, Kanzaki S, Okano HJ, et al. ProinXammatory cytokines expression in noise-induced damaged cochlea. J Neurosci Res. 2006 Mar; 83(4): 575–83.
11. Papp Z, Rezes S, Jókay I, et al. Sensorineural hearing loss in chronic otitis media. Otol Neurotol. 2003; 24(2): 141–144.
12. Shin YJ, Fraysse B, Deguine O, et al. Sensorineural hearing loss and otosclerosis: a clinical and radiologic survey of 437 cases. Acta Otolaryngol. 2001 Jan; 121(2): 200–4.
13. Spandow O, Soderberg O, Bohlin L. Long-term results in otosclerotic patients operated by stapedectomy or stapedotomy. Scand Audiol. 2000; 29: 186–90.
14. Fisch U. Stapedotomy versus stapedectomy 1982. Otol Neurotol. 2009; 30: 1160–5.
15. Skřivan J, Betka J, Kuchař M, et al. Short- and long-term functional results of stapedoplasty (in Czech). Otorinolaryng a Foniat (Prague). 2005; 54(2): 87–90.
16. Bauchet St Martin M, Rubinstein EN, Hirsch BE. High-frequency sensorineural hearing loss after stapedectomy. Otol Neurotol. 2008 Jun; 29(4): 447–52.
17. Strömbäck K, Köbler S, Rask-Andersen H. High frequency hearing followingstapes surgery. Acta Otolaryngol. 2012 Sep; 132(9): 944–50.

18. Satar B, Sen D, Karahatay S, et al. Effect of cochlear reserve on postoperative outcome in otosclerosis. Eur Arch Otorhinolaryngol. 2007; 264: 489–93.
19. Topsakal V, Fransen E, Schmerber S, et al. Audiometric analyses confirm a cochlear component, disproportional to age, in stapedial otosclerosis. Otol Neurotol. 2006; 27: 781–7.
20. Yin X, Stromberg AK, Duan M. Evaluation of the noise generated by otological electrical drills and suction during cadaver surgery. Acta Otolaryngol. 2011; 131: 1132–5.
21. Lundman L, Strömbäck K, Björsne A, et al. Otosclerosis revision surgery in Sweden: hearing outcome, predictive factors and complications. Eur Arch Otorhinolaryngol. 2020 Jan; 277(1): 19–29.
22. Blijleven EE, Wegner I, Tange RA, et al. Revision Stapes Surgery in a Tertiary Referral Center: Surgical and Audiometric Outcomes. Ann Otol Rhinol Laryngol. 2019 Nov; 128(11): 997–1005.
23. Skrivan J, Cada Z, Kluh J, et al. Revision operations after previous stapes surgery for persisting hearing loss. Bratisl Lek Listy. 2014; 115(7): 442–4.
24. Lamblin E, Karkas A, Jund J et al. Is the Carhart notch a predictive factor of hearing results after stapedectomy? Acta Otorhinolaryngol Ital. 2021 Feb; 41(1): 84–90.
25. Carhart R. Clinical application of bone conduction audiometry. Arch Otolaryngol. 1950; 51(6): 798–808.
26. Tonndorf J. Animal experiment in bone conduction: Clinical conclusions. Ann Otol Rhinol Laryngol. 1964 Sep; 73: 658–78.

Visual Acuity Screening of Refugees and Immigrants with a Web-Based Digital Test: A Pilot Study

Minas Bakirtzis[1,*], Eirini Michaleakou[2], Maria-Eleni Martidou[2], Eleni Lahana[2,3], Petros Kostagiolas[2,4], Dimitris Niakas[2,5], Georgios Labiris[1,2]

ABSTRACT

Purpose: To screen visual acuity in two refugee camps in Greece and explore the feasibility of replicating these methods on a nationwide scale.
Methods: Visual acuity was assessed in all participants using web-based Democritus Digital Acuity & Reading Test (DDART). Furthermore, the immigrants responded to a structured questionnaire regarding their demographics and medical history.
Results: A total of 330 adult refugees and immigrants were recruited. A total of 47.3% of the patients had never undergone ophthalmological examination. A significant negative correlation was detected between age ($r = -0.207$, $p < 0.001$) and educational background ($r = -0.135$, $p = 0.014$), suggesting that younger immigrants who had attended compulsory education were more likely to have their eyes checked in their home country. A total of 6.97% of patients presented with impaired vision and were referred for further care. All remote DDART measurements presented no differences from the corresponding hospital-based data in the referred cases.
Conclusions: Visual acuity screening using DDART provides valuable information regarding the visual capacity of refugees. The study outcomes suggest that pilot methods can be replicated on a nationwide scale.
Clinical trials. Gov number NCT05209581; date of registration: January 13, 2022.
This research did not receive any specific grant from funding agencies in the public, commercial, or not-for-profit sectors.
The authors have no funding or conflicts of interest to disclose.
Patients Consent Statement: The patients sign written consent form.

KEYWORDS

refugees; immigrants; visual acuity; DDART; screening

AUTHOR AFFILIATIONS

[1] Medical School, Democritus University of Thrace, Alexandroupolis, Greece
[2] Faculty of Social Sciences, Hellenic Open University, Patras, Greece
[3] Department of Public and One Health, School of Social Sciences, University of Thessaly, Karditsa, Greece
[4] Department of Archives, Library Science and Museology, School of Information Science and Informatics, Ionian University, Corfu, Greece
[5] Medical School, National and Kapodistrian University of Athens, Athens, Greece
* Corresponding author: Democritus University of Thrace, Dragana, Alexandroupolis, 68100, Greece; minas961@hotmail.com

Received: 15 July 2024
Accepted: 3 September 2024
Published online: 18 February 2025

Acta Medica (Hradec Králové) 2024; 67(3): 79–86
https://doi.org/10.14712/18059694.2025.2

INTRODUCTION

Since 2015, the European Union (EU) has faced a challenging migration crisis (1). Millions of immigrants and refugees arrived in several European countries during past years; while political unrest in the Middle East, Africa, and recently in Ukraine suggests that the migration crisis will be escalate in the near future. Greece is the far southeast border of Europe and, traditionally, all major illegal transit routes from the East cross the Greek borders, either at the Aegean Sea or at the Evros river (2). Despite the full implementation of the Operation Poseidon from Frontex with 24/7 Aegean Sea borders surveillance, currently Greece hosts around 120.000 illegal immigrants and refugees in special designed accommodation centers; the majority of them being Afghani, Syrian and Somali (1).

The aforementioned populations are considered vulnerable because they migrate from countries with constrained National Healthcare Systems (NHS) and require both medical screening and care provision. As a result, the Greek NHS faces increased pressure for primary care provision in several remote continental and island areas. Despite the remarkable efforts of the Greek NHS's medical and paramedical staff, the overall care provision of refugees and illegal immigrants is still considered as suboptimal, primarily due to lack of resources and poor collaboration with the several non-governmental organizations that operate at the remote refugee camps (1–4).

Among the fundamental screening examinations for the refugees and the illegal immigrants is the visual acuity (VA), since: a) it reflects potential ocular-related diseases and faults; among them, refractive errors and cataract, b) reflects the sight-threatening impact of systemic diseases like the diabetes mellitus and the systemic hypertension, c) is a direct index of the overall visual performance of the examinee. To our knowledge, no official or unofficial screening program for VA has been implemented for refugees and illegal immigrants in Greece.

Recently, our group developed and validated the Democritus Digital Acuity & Reading Test (DDART) (5–7) which has been accredited by the Hellenic Drug Association as a valid test for clinical and screening purposes, both in conventional and telemedical settings. DDART requires no specialized hardware, while its' multilingual interface and its' advanced features allow any trained operator to provide accurate VA measurements from any remote setting.

Within this context, primary objective of this study was to screen the visual acuity of refugees and illegal immigrants from two camps, both in continental and island Greece and explore the feasibility of a nationwide screening program for refugees' VA assessment based on DDART.

MATERIALS & METHODS

SETTING

This was a pilot, observational study. Protocol adhered to the tenets of the Helsinki Declaration and written informed consent was obtained by all participants. The Research Ethics Committee of Democritus University of Thrace (DUTH) approved the protocol. The study was conducted at the Refugee Accommodation Center in Kavala (RACK), Greece and at the Pre-Removal Detention Center (PROKEKA) in the island of Kos in Greece between January 2022 and April 2022. The official registration number of the study is NCT05209581.

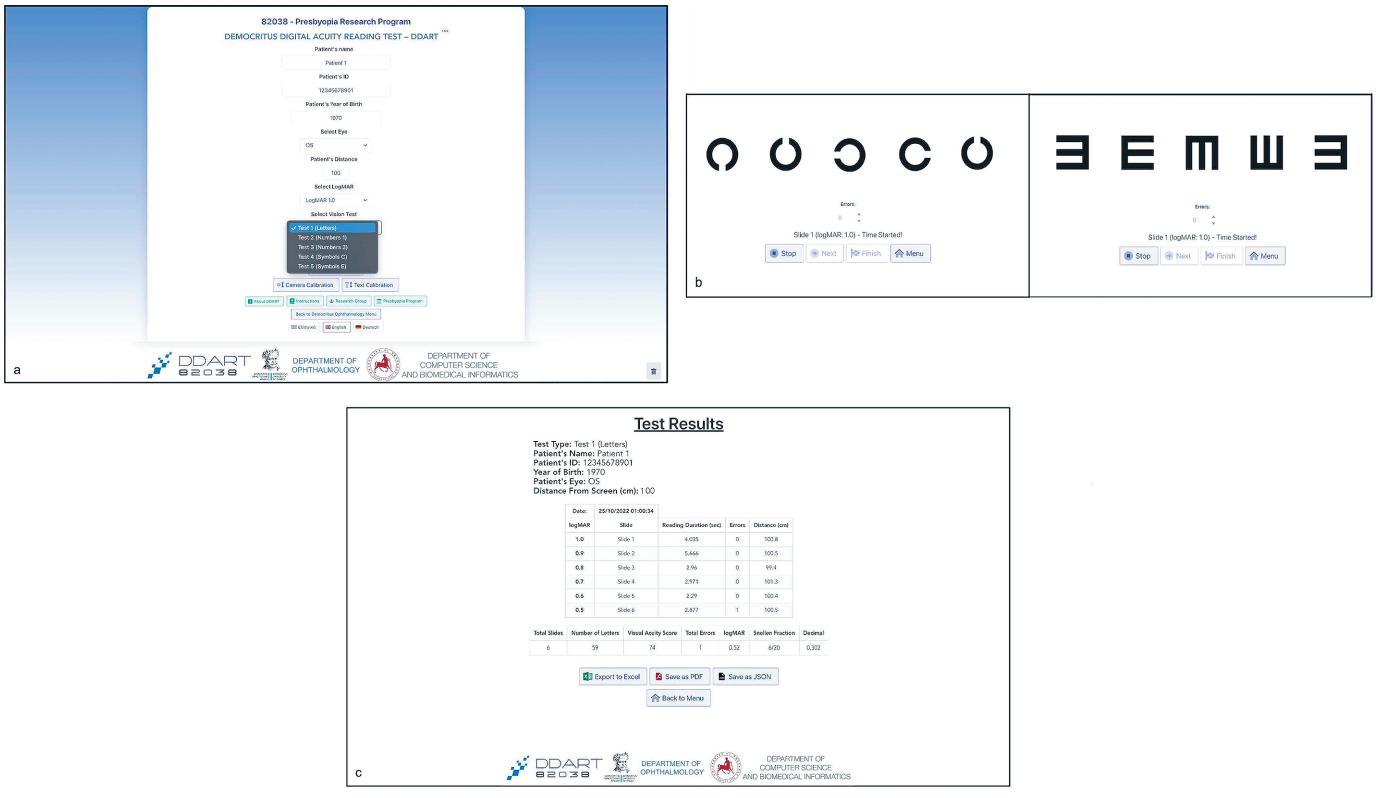

Fig. 1 VA measurement steps in DDART. a. Patient's Demographic Data, b. VA Testing, c. Result Page.

PARTICIPANTS

During participants' recruitment, RACK hosted a total of 400 adult refugees or immigrants originating primarily from Afghanistan and secondarily from Syria, Iran, Iraq, Somalia, Cameroon. PROKEKA hosted 130 adult immigrants originating from Palestine, Yemen, Pakistan, Iraq, Iran, Congo, Somalia, Ivory Coast, Cameroon, West Africa, Tongo, Lebanon, Sierra Leone, Angola, Bangladesh, Sudan and Mali.

Eligibility criteria included age over 18 years and refugee or immigrant status. Exclusion criteria included visual acuity lower than 1.0 logMAR (S.E. = 20/(20*(10^logMAR))), age under 18 years and refugees or immigrants living in the accommodation structures without having the appropriate legal documents.

DATA COLLECTION

Each participant responded to a structured questionnaire with the assistance of certified translators who were assigned by the administrative authorities of the RACK and the PROKEKA, respectively. The questionnaire pertained to the guest's demographics, medical and ophthalmological history. They were also asked if they have ever visited an ophthalmologist/optometrist. The original language of the questionnaire was English and was translated by the translator to each participant's native language.

Following the response to the questionnaire, visual acuity (VA) in each eye was assessed with the DDART(7), as described before, using the Landolt C or Thumbling E charts. For VA measurements we used a 55-inch smart-TV with a resolution of 3840 × 2160 pixels (4K) at a 3 meters distance. In order to assure reliable VA measurements, all researchers that used DDART addressed an online training course and received certification as DDART operators. The VA measurement steps using DDART are presented briefly in Figure 1.

Visual acuity assessment was performed in the same way and under the same conditions for all subjects. The examination was performed in specially designed rooms. The lighting conditions were the same for all subjects, which were verified using the portable Extech Lux Meter EA30 (Extech Instruments Corporation, USA). Examinees' distance from the chart was measured using a laser distance meter (Stanley TLM99s Laser Distance Measurer, Towson, Maryland, USA). The form of the chart used depends on the educational level of the examinee.

STATISTICAL ANALYSIS

A priori power analysis was performed. For an effect size of 0.3, 122 participants would be required for this study to achieve a power of 0.95 at the significance level of 0.05. The data were collected in MS Excel (Microsoft Corp.) and the statistical analysis was performed with Medcalc software version 20.0.0 for Windows (MedCalc Software, Mariakerke, Belgium).

Descriptive statistical analysis was performed. The Shapiro-Wilk test was used to evaluate the normality of the distribution of quantitative variables. In contrast, the chi-squared test was performed to assess and compare qualitative variables. Spearman's rank correlation coefficient was performed for the correlation between non-parametric variables. P values less than .05 were considered statistically significant.

RESULTS

A total of 330 adult refugees and immigrants (200 from the RACK and 130 from PROKEKA; 233 men, 97 women, aged 30 ± 11.5 years) participated in the study. The average VA of the examinees was 0 ± 0.2147 logMAR in the right eye and 0 ± 0.2098 logMAR in the left eye. The participant demographics and VA measurements are shown in Table 1.

Tab. 1 Study participants.

Parameters	Mean ± SD (Range)
Participants (n)	330 (233 men, 97 women)
Eyes (n)	660
Age (years)	30 ± 11.57 (23, 38)
Educational Background [% (n)]	
< Primary School	21.2% (70)
Primary School	32.1% (106)
Secondary School	36.1% (119)
College/University	10.3% (34)
Post Graduate	0.3% (1)
LogMAR right eye	0.0 ± 0.2147 (-0.1, 0.12)
LogMAR left eye	0.0 ± 0.2098 (-0.1, 0.2)

LogMAR = logarithm of the Minimum Angle of Resolution; SD = standard deviation

Participants who reported a diagnosis of eye disease or an optical fault accounted for 17.5% (58 of 330). Reports were primarily refractive errors, with the majority of them, myopia at a rate of 46.7% (28 out of 58) and presbyopia at a rate of 36.7% (22 out of 58). In total, 12.7% (42 of 330) used spectacles, while 4.2% (14 of 330) had been prescribed eye drops. Regarding former ophthalmological examinations, 47.3% (156 out of 330) of the participants had never visited an ophthalmologist/optometrist, while 30.9% (102 out of 330) had at least one ophthalmological

Tab. 2 Ophthalmological History.

Reported disease or fault	Participants (n)
Myopia	28 (46.7%)
Presbyopia	22 (36.7%)
Astigmatism	3 (5%)
Strabismus	3 (5%)
Dry eye	2 (3.3%)
Hyperopia	1 (1.7%)
Uveitis	1 (1.7%)
Last Ophthalmological Visit	
Never	156 (47.3%)
Last 3 years	102 (30.9%)
Last year	53 (16.1%)
Last month	19 (5.8%)

checkup during the past three years. A significant negative correlation was detected between age (r = −0.207, p<.001) and educational background (r = −0.135, p = .014), suggesting that younger immigrants who had attended compulsory education were more likely to have their eyes checked in their home country. However, no significant difference was detected between men and women in any of the parameters evaluated (Table 2).

World Health Organization suggests that VA values above 0.5 logMAR indicate moderate to severe visual impairment (8). 17 participants (5.16%) had VA above 0.5 logMAR. Moreover, 8 participants (2.43%) presented VA differences above 0.4 logMAR. In accordance to the above, study sample was divided into two groups. The first group included participants with normal vision (NVG) and the second group included participants who had either impaired visual acuity (moderate or severe) in at least one eye and / or significant difference in visual acuity between the two eyes (IVG). NVG participants were 93.03% of the sample, while the rest 6.97% populated the IVG (table 3).

Tab. 3 Comparison of groups.

	Group 1 % (n)	Group 2 % (n)
Visual acuity	Normal visual acuity 94.84% (313)	Impaired visual acuity 5.16% (17)
Difference of visual acuity	Difference < 0.4 97.57% (322)	Difference ≥ 0.4 2.43% (8)
Overall	Normal vision 93.03% (307)	Impaired vision 6.97% (23)

Difference = |LogMAR OD – LogMAR OS|

Considering the above data, a correlation was made between the 2nd group and the participants' frequency of visits to an ophthalmologist/optometrist. The analysis showed that out of a total of 23 participants in the group, six had never visited an ophthalmologist/optometrist. In the entire sample, they constituted 1.82%. At the same time, this percentage was correlated with educational background and sex. The results showed that participants with impaired visual acuity who had not visited an ophthalmologist/optometrist had completed primary or secondary school (3 primary school – 3 secondary school), while no clear superiority was found for gender (4 males – 2 females).

Regarding the examination procedure itself, all DDART operators reported no technical problems or other incidences in data collection, other than the case of 30-minute internet connection loss.

DISCUSSION

It is a truism that the medical care of refugees and immigrants is a challenge to the international community and especially to the hosting countries. Due to their compromised living conditions, they present increased healthcare needs (9, 10).

Unfortunately, the overall care provision at the EU refugee camps is still considered as suboptimal. In fact, the majority of care is covered by non-governmental organizations (NGO) (11–13). Despite the efforts of the volunteers of the NGOs and the generous funding from the European authorities, screening programs present questionable efficacy, primarily due to: a) inconsistency in clinical data collection, b) lack or questionable certification of the volunteers who act as clinical data-collectors, c) questionable processing of data the received. To avoid aforementioned inadequacies, we decided to implement a pilot study regarding VA screening in two camps in Greece and explore the potential feasibility to expand it to a nationwide or even European scale.

Within this context, the following prerequisites were addressed:

a) *Consistent data collection methods*. All VA measurements were obtained with the DDART, a high-end, web-based VA test which incorporates several digital enhancements; among them, biometric distance measurement, automatic measurement of the response time, automatic calculation of VA indexes, multilanguage interface that facilitate the examination process and improve consistency and reliability. DDART requires no specialized hardware, other than a high-resolution screen with a webcam and can be accessed from any remote camp with internet connection.
b) *Certification of the DDART operators who act as VA data collectors*. All local DDART operators received full training in DDART operation and the principles of VA examination. DDART certification program is a flexible, multilanguage online course that pertains to the general principles of VA examination, to the DDART's operation as a distance vision test, and to the DDART's operation as a near and intermediate distance vision test.
c) *Automatic calculation and statistical processing of VA measurements*. DDART automatically calculates all distance and near vision VA indexes, so there is no need of complex mathematical calculations from the operator. The VA report of each examinee is exported in pdf, xls and json digital formats. The latter format feeds a web-based database that allows real-time population statistical analysis. Moreover, each report can optionally be linked with the biometric photograph of the corresponding examinee to avoid misidentification.

Regarding the outcomes of present study, the average age of participants was 30 years old. 47.3% of them had never visited an ophthalmologist/optometrist, while 6,97% demonstrated impaired vision and were referred for a full ophthalmological examination and treatment in an ophthalmological department. In all referred cases, VA measurements at the hospital presented no significant differences with the corresponding ones that were received with the DDART. Significant negative correlation was detected between the probability of presenting impaired vision and frequency of former ophthalmological examinations in their home country. The most important of this study was the 1.82% of the whole sample, which had impaired vision and they had never visited an ophthalmologist/optometrist. This proves that 2 out of 100 in this population had unknown impaired vision. This fact demonstrates the increased eye care needs of the refugees.

To our knowledge, this is the first screening study for visual acuity in Greek refugee camps. Relevant literature revealed the following: Yameen et al. study with Syrian participants, reported an average age of 36 years and impaired visual acuity in 19.4% of the sample, which is higher than our 6.97%. In both studies, the most commonly found ocular disorders were the refractive errors (14). Ahmed et al. cohort study in Bangladesh with 68,462 Afghani refugees reported 7.7% visual impairment which is quite similar to our report (15,16). Kaphle et al. screening initiative in Malawi with 635 participants reported a 3.6% of vision impairment. Another interesting finding in Malawi study was that 95% of the participants had never visited an ophthalmologist/optometrist before (17).

Certain limitation of this study was the significant difference regarding the gender of the participants. Furthermore, in this study recruited immigrants from many different countries. Therefore, no definite conclusion can be drawn regarding the eye care needs of the individual origins. The population of Greek immigrant camps changes really fast, so it is difficult to perform an ophthalmic screening based on the origin of the refugees.

CONCLUSION

In conclusion, remote VA screening in Greek refugee and immigrant camps with DDART provided valuable information on the visual acuity of the participants and allowed the prompt identification of those who needed further ophthalmological care. Moreover, DDART's capacity as a validated web-based VA test indicates that it can be used in any nationwide or even European-wide remote screening initiative for vulnerable populations.

ACKNOWLEDGMENTS

- DDART can be accessed from the Democritus University server at https://ddart.med.duth.gr
- DDART – operator certification course can be accessed from the Democritus University Server at http://eddart.med.duth.gr

REFERENCES

1. Yarwood V, Gunst M, Chen CY, et al. A retrospective review of specialist referrals for refugees into Greece's health system: A humanitarian organization's perspective. Avicenna J Med. 2021; 11: 84–92.
2. Gunst M, Jarman K, Yarwood V, et al. Healthcare access for refugees in Greece: Challenges and opportunities. Health Policy. 2019; 123: 818–24.
3. Lebano A, Hamed S, Bradby H, et al. Migrants' and refugees' health status and healthcare in Europe: a scoping literature review. BMC Public Health. 2020; 20: 1039.
4. Bal S, Duckles A, Buttenheim A. Visual Health and Visual Healthcare Access in Refugees and Displaced Persons: A Systematic Review. J Immigr Minor Health. 2019; 21: 161–74.
5. Labiris G, Panagiotopoulou EK, Chatzimichael E, et al. Introduction of a digital near-vision reading test for normal and low vision adults: development and validation. Eye Vis (Lond). 2020; 22: 51.
6. Labiris G, Panagiotopoulou EK, Duzha E, et al. Development and Validation of a Web-Based Reading Test for Normal and Low Vision Patients. Clin Ophthalmol. 2021; 22: 3915–29.
7. Labiris G, Panagiotopoulou EK, Delibasis K, et al. Validation of a web-based distance visual acuity test. J Cataract Refract Surg. 2023 Epub ahead of print.
8. World Health Organization. International Classification of Diseases 11. WHO; 2018 [cited 2022 Oct 13]. Available from: www.who.int/news-room/fact-sheets/detail/blindness-and-visual-impairment.
9. Mattar S, Gellatly R. Refugee mental health: Culturally relevant considerations. Curr Opin Psychol. 2022; 47: 1014–29.
10. Daniel-Calveras A, Baldaquí N, Baeza I. Mental health of unaccompanied refugee minors in Europe: A systematic review. Child Abuse Negl. 2022; 133: 1058–65.
11. Dalla V, Panagiotopoulou EK, Deltsidou A, et al. Level of Awareness Regarding Cervical Cancer Among Female Syrian Refugees in Greece. J Cancer Educ. 2022; 37(3): 717–27.
12. Giannopoulou I, Mourloukou L, Efstathiou V, Douzenis A, Ferentinos P. Mental health of unaccompanied refugee minors in Greece living "in limbo". Psychiatriki. 2022; 33: 219–27.
13. Gelaw Y, Abateneh A. Ocular morbidity among refugees in Southwest Ethiopia. Ethiop J Health Sci. 2014; 24(3): 227–34.
14. Bin Yameen TA, Abadeh A, Slomovic J, Lichter M. Visual impairment and unmet eye care needs among a Syrian adult refugee population in a Canadian city. Can J Ophthalmol. 2020; 55: 137–42.
15. Ahmed M, Whitestone N, Patnaik JL, et al. Burden of eye disease and demand for care in the Bangladesh Rohingya displaced population and host community: A cohort study. PLoS Med. 2020; 17: e1003096.
16. Hussain AE, Al Azdi Z, Islam K, Kabir AE, Huque R. Prevalence of Eye Problems among Young Infants of Rohingya Refugee Camps: Findings from a Cross-Sectional Survey. Trop Med Infect Dis. 2020; 5: 21.
17. Kaphle D, Gyawali R, Kandel H, Reading A, Msosa JM. Vision Impairment and Ocular Morbidity in a Refugee Population in Malawi. Optom Vis Sci. 2016; 93: 188–93.

APPENDICES

Questionnaire

1. Region Country

_____

2. Age

_____

3. Gender

☐ Male ☐ Female

4. Do you have a known eye disease?

☐ Yes _____ ☐ No

5. When was the last visit in an ophthalmologist?

☐ 1 < 1 month ☐ 2 < 1 year ☐ 4 < 3 years ☐ 5 Never

6. Do you use eye drops?

☐ Yes _____ ☐ No

7. Do you wear spectacles?

☐ Yes _____ ☐ No

8. Educational Level ,,,,

Primary School	☐ Yes | ☐ No
Secondary School	☐ Yes | ☐ No
College / University	☐ Yes | ☐ No
Post Graduate	☐ Yes | ☐ No

9. Systematic History

Diabetes Mellitus	☐ Yes | ☐ No
Arterial Hypertension	☐ Yes | ☐ No
Cardiac Disease	☐ Yes | ☐ No
Autoimmune Disease	☐ Yes | ☐ No
Neoplasm	☐ Yes | ☐ No

Other

Fellow _____ / Date _____

ID. _____

Subject _____

STROBE Statement—checklist of items that should be included in reports of observational studies

	Item No.	Recommendation	Page No.	Relevant text from manuscript
Title and abstract	1	(*a*) Indicate the study's design with a commonly used term in the title or the abstract	1	Title
		(*b*) Provide in the abstract an informative and balanced summary of what was done and what was found	2	Summary
Introduction				
Background/rationale	2	Explain the scientific background and rationale for the investigation being reported	2	Introduction
Objectives	3	State specific objectives, including any prespecified hypotheses	2-3	Introduction
Methods				
Study design	4	Present key elements of study design early in the paper	3-4	Methods
Setting	5	Describe the setting, locations, and relevant dates, including periods of recruitment, exposure, follow-up, and data collection	3	Methods
Participants	6	(*a*) *Cohort study*—Give the eligibility criteria, and the sources and methods of selection of participants. Describe methods of follow-up *Case-control study*—Give the eligibility criteria, and the sources and methods of case ascertainment and control selection. Give the rationale for the choice of cases and controls *Cross-sectional study*—Give the eligibility criteria, and the sources and methods of selection of participants	3-4	Methods
		(*b*) *Cohort study*—For matched studies, give matching criteria and number of exposed and unexposed *Case-control study*—For matched studies, give matching criteria and the number of controls per case		
Variables	7	Clearly define all outcomes, exposures, predictors, potential confounders, and effect modifiers. Give diagnostic criteria, if applicable	4-5	Methods
Data sources/ measurement	8*	For each variable of interest, give sources of data and details of methods of assessment (measurement). Describe comparability of assessment methods if there is more than one group	4-5	Methods
Bias	9	Describe any efforts to address potential sources of bias	4-5	Methods
Study size	10	Explain how the study size was arrived at	5	Methods
Quantitative variables	11	Explain how quantitative variables were handled in the analyses. If applicable, describe which groupings were chosen and why	4-5	Methods
Statistical methods	12	(*a*) Describe all statistical methods, including those used to control for confounding	5	Methods
		(*b*) Describe any methods used to examine subgroups and interactions	5	Methods
		(*c*) Explain how missing data were addressed	5	Methods
		(*d*) *Cohort study*—If applicable, explain how loss to follow-up was addressed *Case-control study*—If applicable, explain how matching of cases and controls was addressed *Cross-sectional study*—If applicable, describe analytical methods taking account of sampling strategy		
		(*e*) Describe any sensitivity analyses		
Results				
Participants	13*	(a) Report numbers of individuals at each stage of study—eg numbers potentially eligible, examined for eligibility, confirmed eligible, included in the study, completing follow-up, and analysed	6	Results
		(b) Give reasons for non-participation at each stage	6	Results
		(c) Consider use of a flow diagram		
Descriptive data	14*	(a) Give characteristics of study participants (eg demographic, clinical, social) and information on exposures and potential confounders	6-9	Results
		(b) Indicate number of participants with missing data for each variable of interest	6-9	Results
		(c) *Cohort study*—Summarise follow-up time (eg, average and total amount)	6-9	Results
Outcome data	15*	*Cohort study*—Report numbers of outcome events or summary measures over time	6-9	Results
		Case-control study—Report numbers in each exposure category, or summary measures of exposure		
		Cross-sectional study—Report numbers of outcome events or summary measures		
Main results	16	(*a*) Give unadjusted estimates and, if applicable, confounder-adjusted estimates and their precision (eg, 95% confidence interval). Make clear which confounders were adjusted for and why they were included	6-9	Results
		(*b*) Report category boundaries when continuous variables were categorized	6-9	Results
		(*c*) If relevant, consider translating estimates of relative risk into absolute risk for a meaningful time period		

Continued on next page

Other analyses	17	Report other analyses done—eg analyses of subgroups and interactions, and sensitivity analyses	6-9	Results
Discussion				
Key results	18	Summarise key results with reference to study objectives	9-11	Discussion
Limitations	19	Discuss limitations of the study, taking into account sources of potential bias or imprecision. Discuss both direction and magnitude of any potential bias	11	Discussion
Interpretation	20	Give a cautious overall interpretation of results considering objectives, limitations, multiplicity of analyses, results from similar studies, and other relevant evidence	9-11	Discussion
Generalisability	21	Discuss the generalisability (external validity) of the study results	9-11	Discussion
Other information				
Funding	22	Give the source of funding and the role of the funders for the present study and, if applicable, for the original study on which the present article is based		

*Give information separately for cases and controls in case-control studies and, if applicable, for exposed and unexposed groups in cohort and cross-sectional studies.

Note: An Explanation and Elaboration article discusses each checklist item and gives methodological background and published examples of transparent reporting. The STROBE checklist is best used in conjunction with this article (freely available on the Web sites of PLoS Medicine at http://www.plosmedicine.org/, Annals of Internal Medicine at http://www.annals.org/, and Epidemiology at http://www.epidem.com/). Information on the STROBE Initiative is available at www.strobe-statement.org.

Forecasting with Excel

Victor Grech[1,*]

ABSTRACT
Introduction: Time series analysis is used by statisticians to make predictions from time-ordered data. This is crucial for planning for the future. The inclusion of little-known forecasting function in Excel™ has brought this type of analysis within the ability of less mathematically sophisticated individuals, including doctors. There are two main models for time series analysis: ARIMA (Autoregressive Integrated Moving Average) and exponential smoothing. This paper will demonstrate how the ubiquitous Excel facilitates a little-known sophisticated forecasting technique that employs the latter and presents a facilitating spreadsheet.
Methods: Excel's FORECAST.ETS function was invoked with supporting macros.
Results: A bespoke spreadsheet was created that would prompt for data to be pasted in columns A and B, formatted as a valid date in A and data in B. After error trapping and a horizon date, the FORECAST.ETS function calculates forecasts with 95% CI and a line graph. The FORECAST.ETS.CONFINT was also invoked using a macro to obtain a 95, 96, 97, 98 and 99% confidence intervals table.
Discussion: Forecasting is vital in all fields, including the medical field, for innumerable reasons. Statisticians are capable of far more sophisticated time series analyses and techniques and may use multiple techniques that are beyond the competence of ordinary clinicians. However, the sophisticated Excel tool described in this paper allows simple forecasting by anyone with some knowledge of this ubiquitous software. It is hoped that the spreadsheet included with this paper helps to encourage colleagues to engage with this simple-to-use Excel function.

KEYWORDS
health services needs and demand; statistics & numerical data; trends; health Workforce; models; statistical; Excel; forecasting; exponential smoothing; holt-winters test

AUTHOR AFFILIATION
[1] Mater Dei Hospital, Malta
* Paediatric Dept, Mater Dei Hospital, Malta; victor.e.grech@gov.mt

Received: 13 April 2024
Accepted: 14 October 2024
Published online: 18 February 2025

Acta Medica (Hradec Králové) 2024; 67(3): 87–90
https://doi.org/10.14712/18059694.2025.3

INTRODUCTION

Time series analysis and forecasting techniques are used by statisticians and data scientists to make predictions from time-ordered data. This type of data consists of a series of observations over time, such as patient admissions, weather patterns, or sales figures. Forecasting is crucial for planning, allowing the anticipation and preparation for future trends, opportunities, and challenges and for providing benchmarks against which performance can be compared. Forecasting also allows correct resource allocation which may be financial, manpower, and materials, thereby minimising or possibly eliminating shortages or surpluses (1).

Forecasting is vital in medicine for many reasons. It is crucial in resource allocation, predicting admissions, disease outbreaks, or surgical procedures, allowing hospitals and healthcare facilities to efficiently allocate resources such as hospital beds, staff, medications, and equipment. By forecasting patient volumes and case types, hospitals and healthcare facilities can better plan staffing requirements at any given time. Forecasts also predict demand for medical supplies such as medications, vaccines, and medical equipment, managing inventory levels, reducing wastage, and ensuring availability during emergencies or spikes in demand. Forecasting may also help to predict disease outbreaks based on historical data, environmental factors, and population trends, allowing early intervention/prevention and resources allocation to control spread. This includes public health preparedness for pandemics, natural disasters, or bioterrorism events by estimating healthcare demands and required resources should such calamities occur. With regard to treatment, forecasting may assist in planning treatment options for patients based on predicted outcomes, thus optimizing care pathways, and ultimately improving patient outcomes. Forecasting may also predict readmission rates, complications, and disease progression, allowing for the preparation of personalized, timely interventions.

Forecasting may also be useful in clinical research, in clinical trials for example, by estimating patient recruitment rates and disease progression, thus helping to plan studies more effectively. Ultimately, forecasting can help to optimise cost management and reduce waste in healthcare services, a universal problem due to ever-increasing demands with finite budgets, a quandary that threatens the viability and sustainability of medical systems worldwide.

A little-known forecasting function in Excel™ has brought this type of analysis within the ability of mathematically unsophisticated individuals, including doctors.

Time series analysis entails the usual steps in data collection and data pre-processing to ensure that the data to be analysed is clean and with the least possible missing values, outliers, and other anomalies. It is also always wise to perform an initial exploratory data analysis to understand the dataset's underlying patterns, and plotting the data is almost a mandatory step (2). A time series analysis is characterised by the following patterns or components:

Level represents the baseline value of the data and is updated at each step by combining the observed value with the estimated level from the previous time step. It thus represents the long-term average of the dataset.

Trend represents the underlying long-term trend direction and rate of change in the data, without the inclusion of seasonal fluctuations (level/upward/downward).

Seasonality refers to regular, predictable patterns that repeat at fixed intervals within a year. These patterns may be daily, monthly, quarterly, or yearly.

Cyclicity refers to fluctuations that occur over an extended period, often more than a year, and are not tied to specific seasons. Unlike seasonal component/s, cyclical component/s do not have fixed periodicity.

The irregular(residual/noise) component consists of random fluctuations or noise in the data that cannot be explained by the above and includes unpredictable events, measurement errors, or other irregular influences. All these components interact to produce the eventual observations/dataset. The data can therefore also be decomposed from a time series into these individual constituents to better understand the structure and behaviour of the time series. and hence facilitate forecasting. There are two main models for time series analysis.

ARIMA

ARIMA (Autoregressive Integrated Moving Average) techniques are widely used in time series forecasting due to their ability to handle various types of data patterns. The method combines three critical components: the autoregressive (AR) component, the moving average (MA) component, and an integrated (I) aspect. The autoregressive element implies that the current data point is influenced by its preceding values, making it a powerful tool for identifying trends and patterns over time. Essentially, AR models explain the variability of the present value based on a weighted sum of prior data points. This relationship allows ARIMA to capture momentum and fluctuations within a time series. The moving average (MA) component relies on a sequence of past forecast errors to correct the model. By taking a linear combination of several points from the recent past, the model reduces noise, smoothing out short-term variations and allowing for a more accurate prediction of future values. This method captures short-term shocks and fluctuations by adjusting predictions based on previous errors, making the model more responsive to sudden changes in data. The "Integrated" part of ARIMA refers to the process of differencing the data to make it stationary. Time series data often exhibit trends or seasonality that ARIMA models need to eliminate through differencing. This mathematical transformation ensures that any trend is removed, and the data's mean and variance remain constant over time. By applying this process, ARIMA models can adapt to datasets with a wide variety of behaviors, including those with long-term trends or seasonal effects. ARIMA's versatility stems from its capacity to combine these three elements – autoregression, moving averages, and integration – into a single, cohesive framework. As a result, ARIMA models are highly adaptable to different types of data, making them suitable for applications ranging from economic forecasting to environmental

data analysis. They are flexible enough to handle datasets with missing values or irregular intervals, and they exhibit robustness in the face of outliers, allowing for reliable forecasting even when dealing with complex real-world data. Although Excel does not natively support ARIMA modeling, it is possible to apply these techniques using specialized add-ins (3, 4).

EXPONENTIAL SMOOTHING

Exponential methods smooth datasets by using exponential functions such that the weighting of individual datapoints on subsequent data exponentially decreases over time, giving more weight to more recent observations. Techniques include simple exponential smoothing, double exponential smoothing (Holt's method), and triple exponential smoothing (Holt-Winters method) with the latter taking into account level, trend and seasonality (5–8). In brief, this technique identifies the level, trend, and seasonal components, updates each of these at each time step by exponential smoothing and uses these updated elements to forecast future steps. The method requires the entry of parameters such as smoothing coefficients and the lengths of seasonal periods. However, the software used to perform this test may be able to self-optimise these parameters for best fit.

PROS AND CONS

The Holt-Winters technique is arguably better at capturing and forecasting seasonality, and is simpler to use, with fewer parameters needing to be input. It is also generally more accurate for short-term predictions. Furthermore, an ARIMA forecast is often a straight line devoid of patterns, showing the mathematical model of best fit unless a more complex SARIMA (Seasonal Autoregressive Integrated Moving Average) is used (an extension of the non-seasonal ARIMA model, designed to handle data with seasonal patterns), while a Holt-Winters analysis will create forecasts that closely resemble the original data. In practice, the choice between the two depends on the properties of the dataset and the horizon required to forecast to (9, 10). Vis-à-vis implementing ARIMA analysis in Excel, the utilisation of an add-in to Excel may slow down Excel during daily use.

For complex analyses, it may be necessary to use multiple methods including hybrid approaches, but this is beyond the scope of this paper. Machine learning models and artificial intelligence are also being harnessed, but these are also beyond the scope of this paper.

This paper will demonstrate how the ubiquitous Excel contains a little known and little appreciated but quite sophisticated forecasting technique that employs the Holt-Winters method. This paper also presents a spreadsheet that facilitates the software's performance of this test.

METHODS

EXCEL FORECAST.ETS FUNCTION

Excel's FORECAST.ETS function (version 2016 and above) forecasts using the so-called AAA (additive error, additive trend, and additive seasonality) version of the Exponential Triple Smoothing (ETS) algorithm.

The syntax is: FORECAST.ETS(target_date, values, timeline, [seasonality], [data_completion], [aggregation])

Alternatively, the function can be accessed without invoking the function directly from the Data ribbon, in the Forecast group: activate Forecast Sheet. The user is asked to set the forecast date horizon and choose between a line chart or a column chart for graphical output which is also produced with 95% confidence intervals. The latter can be varied at this point as well (11).

This function requires data at regular intervals (hourly, daily, monthly, quarterly, yearly) and is best suited for non-linear data with seasonal or other repetitive pattern/s. When the function fails to detect a pattern, the forecast output is linear. The function is robust up to a point with incomplete datasets, where up to 30% of data points may not available.

RESULTS

A spreadsheet was created that would prompt for data to be pasted in columns A and B, formatted as a valid date in column A and data in column B. The sheet also finds and displays the date in the last row of column A, and the user is expected to input a valid date to forecast to. A macro was created that performed error trapping and gives the user appropriate prompts (e.g., invalid forecast date format or date to forecast is less than the last date in the dataset). The macro invokes the FORECAST.ETS function with the following (default) parameters, with the calculation of 95% CI for the forecast dates and the creation of a line graph with 95% CI.

ActiveWorkbook.CreateForecastSheet Timeline:=Sheets("Forecast sheet").Range("A1:A" & lr), Values:=Sheets("Forecast sheet").Range("B1:B" & lr), ForecastEnd:=lrend, ConfInt:=0.95, Seasonality:=1, ChartType:=xlForecastChartTypeLine, Aggregation:=xlForecastAggregationAverage, DataCompletion:=xlForecastDataCompletionInterpolate, ShowStatsTable:=True

In this macro, lr is the last column row (for columns A and B), a variable which is obtained by using another function, and this therefore ensures that the entire data range is captured by the macro and used for analysis, whatever the column length.

The calculation of confidence intervals for the predicted forecast at each future date is also possible at any desired level with this function. For monthly data, the FORECAST.ETS function is therefore used for the actual prediction for a 10 year period and the FORECAST.ETS.CONFINT(range, CI) is used to obtain 95, 96, 97, 98 and 99% confidence intervals. These are, individually (at every next predicted value), added to and subtracted from the FORECAST.ETS output, allowing the calculation of confidence intervals for each of these five levels. A macro was created to import the dataset into this sheet so as not only to use the Excel standard function and output (table and graph) but also to tabulate these five confidence levels. This allows users to identify any outlier/s in the dataset by comparing to the sheet's output, and by locating the divergence away

from the estimated average, be able to calculate p values based on how many percentiles the outlier/s are from the estimated mean.

The sheet is available for download from this location: https://tinyurl.com/3nbf9rba

DISCUSSION

It must be reiterated that statisticians and data scientists are capable of far more sophisticated time series analyses and techniques and indeed, may use multiple techniques that are beyond the competence of ordinary clinicians (12–14). Excel natively performs forecasting using the Holt-Winters test and the Excel tool described in this paper allows simple forecasting by anyone with some knowledge in using Excel. It is hoped that the spreadsheet included with this paper helps to encourage colleagues to engage with this simple-to-use Excel function.

In summary, forecasting provides valuable insights into the future, enabling better decision-making, risk management, and planning across various domains. It allows individuals and organizations to anticipate change, adapt to new circumstances, and thrive in an uncertain world, and this software may be of help.

CONFLICTS OF INTEREST

The author runs the Write a Scientific Paper course (WASP), for which the spreadsheet presented in this paper was created.

REFERENCES

1. Montgomery DC, Jennings CL, Kulahci M. Introduction to Time Series Analysis and Forecasting. New York: John Wiley & Sons, Ltd, 2015.
2. Grech V. Write a Scientific Paper (WASP): Effective graphs and tables. Early Hum Dev; 134. Early Hum Dev. 2019 Jul: 134: 51–54.
3. Box GEP, Jenkins GM, Reinsel GC, et al. Time Series Analysis: Forecasting and Control. New York: John Wiley & Sons, Ltd, 2015.
4. Zaiontz C. Real Statistics Using Excel, www.real-statistics.com (2024).
5. Brown RG. Exponential Smoothing for Predicting Demand. Cambridge (MA): Little, 1956.
6. Holt CC. Forecasting trends and seasonals by exponentially weighted averages. O.N.R. Research Memorandum, 1957.
7. Winters PR. Forecasting sales by exponentially weighted moving averages. Manage Sci. 1960; 6: 324–342.
8. Holt CC. Forecasting seasonals and trends by exponentially weighted moving averages. Int J Forecast. 2004; 20: 5–10.
9. Chaurasia V, Pal S. Application of machine learning time series analysis for prediction COVID-19 pandemic. Res Biomed Eng. 2020; 1–13.
10. Mgale YJ, Yan Y, Timothy S. A comparative study of ARIMA and Holt-Winters exponential smoothing models for rice price forecasting in Tanzania. Open Access Libr J. 2021; 8: 1–9.
11. Rahardja D. Statistical Time-Series Forecast via Microsoft Excel (FORECAST. ETS) Built-In Function. J Res Appl Math. 2021; 7: 69–73.
12. Vieira A, Sousa I, Dória-Nóbrega S. Forecasting daily admissions to an emergency department considering single and multiple seasonal patterns. Healthc Anal. 2023; 3: 100146.
13. Klein B, Zenteno AC, Joseph D, et al. Forecasting hospital-level COVID-19 admissions using real-time mobility data. Commun Med. 2023; 3: 25.
14. Zhou L, Zhao P, Wu D, et al. Time series model for forecasting the number of new admission inpatients. BMC Med Inform Decis Mak. 2018; 18: 39.

Colloid Cyst of the Third Ventricle: A Case Report

Aleš Kopal[1], Jiří Preis[2], Leoš Ungermann[3], Edvard Ehler[1,*], Ivana Štětkářová[4]

ABSTRACT
Colloid cyst of the third ventricle (CC) represents approximately 1% of intracranial tumours and 20% of intraventricular tumours. CC usually occurs between 20 and 50 years of age. During the first decade of life, it is diagnosed very rarely (1–2%). It can be most commonly found in the anterior part of the third ventricle at the foramen of Monro (1). It is often visualised during the computed tomography (CT) examination as a hyperdense focal lesion, it has variable change of the signal during magnetic resonance imaging (MRI) (2). CC has a benign character, however, a strategic position which may lead to acute hydrocephalus, intracranial hypertension syndrome, consciousness disorder, and even sudden death. This peracute hydrocephalus is an indication to an acute neurosurgical procedure (3).

KEYWORDS
colloid cyst; intracranial hypertension; malignant brain edema; external ventricular drainage

AUTHOR AFFILIATIONS
[1] Neurologic Department of Faculty of Health-Care Studies University, Pardubice, and Regional Hospital Pardubice, Czech Republic
[2] Neurosurgery Department of Faculty of Health-Care Studies University, Pardubice, and Regional Hospital Pardubice, Czech Republic
[3] Radiodiagnostic Department of Faculty of Health-Care Studies University, Pardubice, and Regional Hospital Pardubice, Czech Republic
[4] Neurologic Department of University Hospital Královské Vinohrady Prague and 3rd Medical Faculty Charles University, Czech Republic
* Corresponding author: Department of Neurology, Faculty of Health-Care Study, Pardubice University, District Hospital Pardubice, Czech Republic; edvard.ehler@nempk.cz

Received: 11 December 2024
Accepted: 27 August 2024
Published online: 18 February 2025

Acta Medica (Hradec Králové) 2024; 67(3): 91–95
https://doi.org/10.14712/18059694.2025.4

CASE REPORT

A 30-year-old, previously healthy man developed headache with a maximum in the frontal region 3 weeks ago. The pain had a tension character, and the patient did not report any provoking factor. The headaches significantly deteriorated after one week, he still woke up at night due to pain, was unsafe when walking, eventually preventing him from walking even to the toilet. He started to be drowsy and was transferred to neurology at night in this condition. He vomited repeatedly at the outpatient clinic. His psychomotor rate was slower upon admission, he cooperated actively; his pupils were equal, with preserved photoreaction, abdominal reflexes were low, without irritation pyramidal symptoms on the lower limbs, no nuchal rigidity, Lasegue was negative, standing position very unstable, BP 205/105, HR 56/min, regular. CT examination of the brain and CT angiography of carotids and vertebral arteries reported a hyperdense spherical focal lesion of 18 × 26 mm in the midline in area of the 3rd ventricle, with dilatation of lateral ventricles to 22 mm, small hypodense rims at the occipital corners with the infiltration of cerebrospinal fluid. There was no dilatation of the 3rd and 4th ventricles. Supratentorial subarachnoid cisterns were faded, basal cisterns were preserved (Figure 1). Angiography of cerebral arteries was normal. He was admitted to the neurological ICU, the anti-oedematous treatment (mannitol, NaCl 10% 20 ml) was initiated immediately, and a neurosurgeon was consulted. Laboratory levels revealed no clear deviations. Ophthalmological examination was acutely performed, revealing fundus congestion with haemorrhages. However, generalized epileptic paroxysm manifested at the same time with the subsequent development of coma. Vomiting of the gastric content occurred again. Brief external cardiac massage was performed within the resuscitation care, the patient was subsequently intubated and artificial pulmonary ventilation was initiated. He was subsequently transferred to the surgical theatre to undergo acute external ventricular drainage. A follow-up brain CT scan was additionally performed during transfer. At arrival to the surgical theatre, his pupils were not round bilaterally; opening pressure of the introduced drainage was 30 cm of the water column, fluid was clear. After introduction of ventricular drainage, the patient was handed over to the care of the anaesthesiology-resuscitation department.

Fig. 1 Initial CT examination.

Dilatation of lateral ventricles and faded subarachnoid space associated with slightly hyperdense spherical expansion of the 3rd ventricle.

Tab 1 Course of patient with colloidal cyst nad peracute syndrom of intracranial hypertension.

9. 12. 2022	Headache, worsening
16. 12. 22 02:35	Neurological examination because of increasing headache, then weakness, sedation, at emergency he vomitted
04:10	Head CT and then CT angiography
04:20	Admission to neurological ICU – antiedematous medication
04:30	Neurosurgical examination – plan of EVD, before surgery – CT control, ophthalmological examination and continuing in antiedematous therapy
04:45	Ophthalmological examination
05:03	Epileptic paroxysm with subsequent short resuscitation, then intubation and arteficial ventilation
06:38	Head CT control – extincted cysterns, increased hydrocephalus
07:00	Mydriatic pupils
07:10	Beginning of surgery – CSF, leaking with increased pressure (30 mm H2O)
07:30	Induced EVD, end of surgery
07:35	Transfer to Anesthesiology, anisocoria – right 5mm and left 3 mm
09:07	Head MRI, induced EVD, diffuse brain edema

Brain MRI was performed (Figure 2). Figure 3 short, transient clinical improvement (for several hours) was followed by a period of hypertension that was difficult to control, with unilateral mydriasis on the right, due to which further acute CT scan was performed (Figures 4, 5). Faded differentiation between the grey and white matter was obvious here, with insignificant haemorrhage into the ventricular system, and a virtually collapsed ventricular system. During the following several hours, bilateral mydriasis developed, followed by brainstem areflexia within 24 hours from the initial examination. CT angiography revealed no filling of cerebral vessels except for a questionable M1 segment on the left. The patient was handed over to the transplant programme.

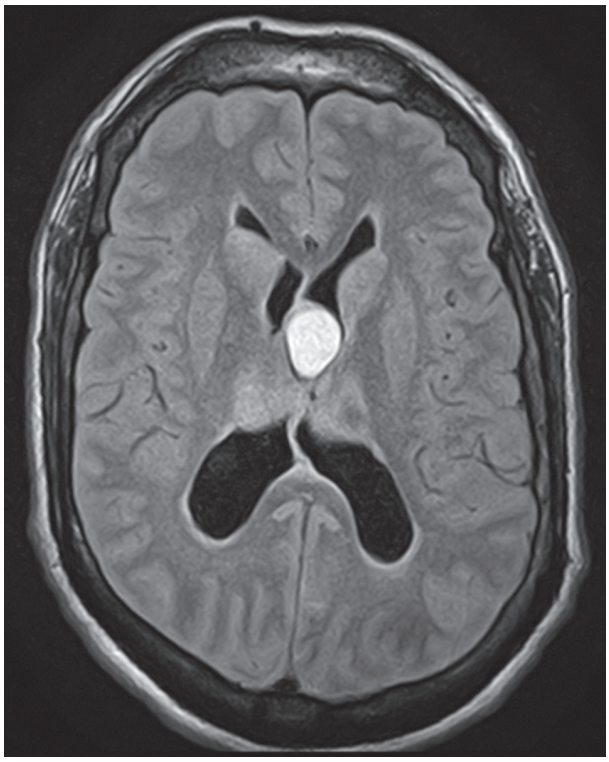

Fig. 2 MRI examination – FLAIR sequence.

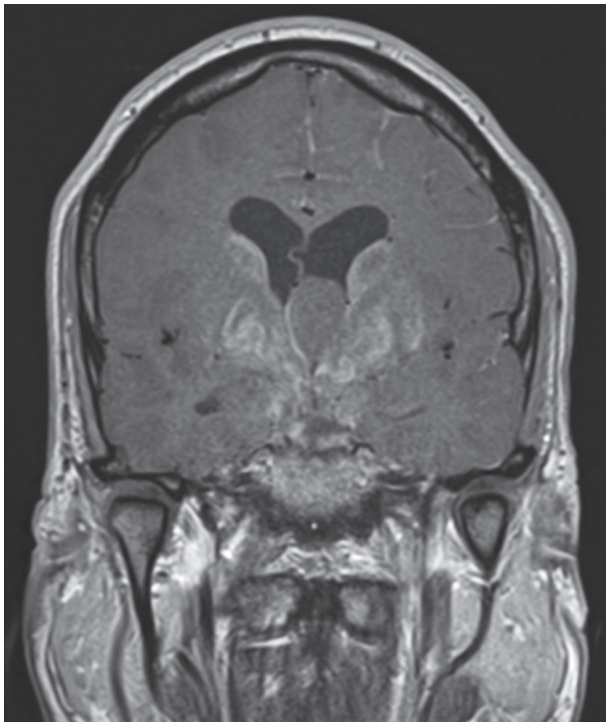

Fig. 3 MRI examination: contrast-enhanced T1-weighted images in the coronary plane.

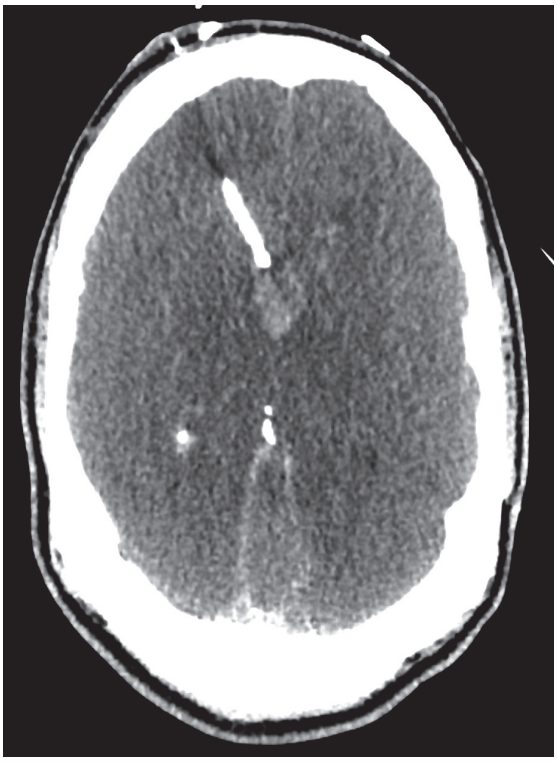

Fig. 4 Follow-up CT examination after 34 hours.

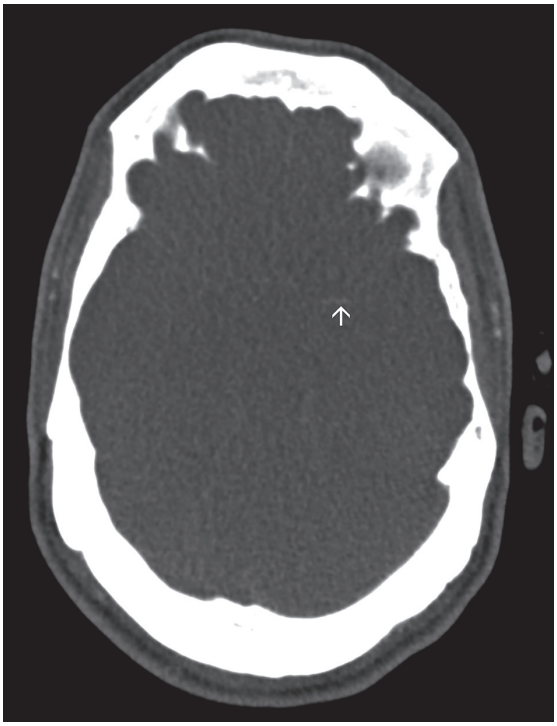

Fig. 5 CT angiography of the carotid circulation.

Dilatation of lateral ventricles with an image of active hydrocephalus associated with a hyperintense lesion of the 3rd ventricle, a typical image of the colloid cyst at the top of the 3rd ventricle.

The lesion of the 3rd ventricle without enhancement after administration of contrast substance. However, pathological enhancement of both thalami and basal ganglia is obvious with diffuse oedema and impaired blood-brain barrier.

Image of diffuse cerebral oedema with faded differentiation between the grey and white cerebral matter. Ventricular drainage on the right in the frontal region.

Only poor MCA filling obvious intracranially on the left (marked with an arrow).

DISCUSSION

Opinions on the origin of CC and especially on the tissue type it comes from have gone through long evolution. In the 1920s, there was discussion about paraphysis, the embryonic tissue from which CC could arise. In the 1950s, ependyma of the third ventricle was considered. Then, there was a theory of a neuroepithelial origin. The epithelium in the choroid plexus and ependyma of the 3rd ventricle share the same origin – the neuroepithelium – and CC most probably forms from this tissue. Current microscopic demonstration of cilia on these epithelial cells and the presence of goblet cells, demonstration of desmosomes points to significant resemblance of the CC structure to respiratory epithelium. Hence, there is considerable similarity with Rathke's cyst (4).

The genetic theory is the result of epidemiological studies where CC has occurred in siblings (especially females) and also in twins (1).

Cardiovascular symptoms occur quite commonly. It is a myocardial contractility disorder (stunned myocardium), associated with pulmonary oedema and heart failure. There was a case report of a 29-year-old woman admitted due to hypertension, tachycardia, and pulmonary oedema. She had significant elevation of cardiac markers in laboratory collections. The transthoracic ECHO examination revealed global hypokinesia and a drop in ejection fraction to 30–35%. There was no diastolic function disorder. Myocardial function also improved after endoscopic CC excision. In pathogenesis of cardiac dysfunction, authors emphasize pressure of growing CC on hypothalamic cardiovascular regulatory centres (3).

The incidence rate of CC is thought to be even lower at ≈0.9 per million. The most common clinical symptom of CC is headache (68–100%); there are typical attacks, lasting for seconds to minutes. However, the duration and intensity of pain is variable depending on the position of the head; worse when sitting upright and improved when lying supine (2). Other symptoms include nausea, vomiting, visual disturbances, and ataxia of the standing position and gait (5). Urinary incontinence, epileptic seizures, falls, sudden death may occur. Although this is a benign process, the risk of sudden neurological deterioration or death caused by colloid cysts is 3% to 35%.

Hydrocephalus (in 99%) is associated with higher probability of death, compared to patients without hydrocephalus. Patients presenting with cyst apoplexy have a high mortality rate (50%), with an average cyst size of 2.5 cm. Mortality is generally higher in women, even with a smaller CC size (2).

Papilledema occurs in up to 57% of patients. Based on a study of 140 patients, authors report that patients without congestion have higher probability of death. However, this is rather related to activity of physicians when activity is lower in patients without congestion (6).

The mechanism of sudden decompensation or death is still controversial. Various theories have been proposed. A possible mechanism is pressure of the cyst on the hypothalamus, resulting in the disruption of autonomic cardiac reflex control, leading to acute cardiac arrest, with or without a pre-existing cardiac disease. Another possible mechanism is based on the relative movement of the cyst on its pedicle with attachment to the tela choroidea, causing intermittent obstruction of the foramen of Monro and sudden intracranial hypertension. Another mechanism is acute haemorrhage in the cyst, causing progressive expansion of the cyst and subsequent obstruction of the foramen (7).

Conservative care is recommended only for clinically stable patient. Cerebrospinal fluid diversion, open surgical approaches, and neuroendoscopy have been applied to the management of colloid cysts (11). The conservative approach in asymptomatic patients is based on head position elevated to 30 degrees, securing of the airways, relaxation, sedation, serum osmolality 295–305 mosm, control of hypertension, maintaining central perfusion pressure above 60 mmHg, normothermia, use of hyperosmolar solutions. Acute external drainage is indicated in severe and rapidly progressing cases.

Surgical treatment of colloid cysts include craniotomy with excision via transcallosal or transcortical route, endoscopic removal, or stereotactic aspiration, and external ventricular drains (or rarely bilateral drains) could also be performed as bridge therapy in life-threatening hydrocephalus (12). External ventricular drainage (EVD) enables the monitoring of intracranial pressure, reduction of the cerebrospinal fluid volume, and temporary treatment of intracranial hypertension. Another option is surgical reduction of the enlarged volume (usually a tumour or haematoma) responsible for the growth of intracranial pressure. The neurosurgeon may opt for decompressive craniectomy in certain cases (6).

This case report describes an acute condition (with a rapidly deteriorating clinical condition and limited options for conservative management), requiring urgent management to affect intracranial hypertension and focus on its cause – introduction of external ventricular drainage. The important role of cerebrospinal fluid on the development of malignant brain oedema is an important pathogenic mechanism in acute obstructive hydrocephalus leading to bad prognosis (8, 13).

Surgical management depends on the fact of whether the colloid cyst is found incidentally or is symptomatic and whether risk factors are present. High mortality rate was observed in patients with neurological deficits. The mortality rate is close to 100% without surgical intervention. Mortality rate reaches only 48% in patients who underwent a surgical procedure (6). Acute conditions are always managed by emergent procedures -external ventricular drainage and cyst resection is primarily approached only rarely (9). After ruling out an acute condition, the colloid cyst may be treated using various surgical methods. For this definitive treatment the approach type is chosen according to the location and size of the cyst in the third ventricle. Transcortical approach using endoscopic technique and navigation is currently utilised. Previously used stereotactic aspiration of the cyst is of marginal use (10).

In our patient with peracute development of intracranial hypertension with biventricular hydrocephalus and malignant brain edema the brain CT and then CT angiography were completed. Because further worsening of consciousness and symptoms with bilateral mydriasis the

neurosurgeon (and neurologist on ICU) insisted on further brain CT to diagnose the evolving pathology, that causes the clinical worsening.

CONCLUSION

It is necessary to consider the risk of the malignant progress (MRI scale) in CC cases to improve the prognosis of patients with CC and peracute intracranial hypertension syndrome (due to biventricular hydrocephalus associated with development of malignant brain oedema). The incidence of peracute progress of intracranial hypertension syndrome requires a rapid diagnosis (CT, MRI) and acute consultation of a neurosurgery workplace. The primary logical surgical solution is introduction of external ventricular drainage and administration of antioedematous treatment. On the example of our patient, we are showing pitfalls of CC management, with a high mortality rate despite rapid diagnosis and treatment.

REFERENCES

1. Niknejad HR, Samii A, Shen SH, Samii M. Huge familial colloid cyst of the third ventricle: An extraordinary presentation. Surg Neurol Int. 2015; 6: S349–53.
2. Al-Sharydan AM, Al-Sahubani SS, Al-Abdulwahhab AH, Al-Aftan MS, Gashgari AF. A unique finding of cavum velum interopositum colloid-like cyst and literature review of a commonplace lesion in an uncommon place. Int J Gen Med. 2018; 11: 301–305.
3. Ayasa M, Shaikh N, Marcus MAE. A 3rd ventricular colloid cyst causing acute hydrocephalus with stunned myocardium: A case report. Qatar Med J. 2020 Nov 12; 2020(2): 28.
4. Khan M, Gardezi SA, Nangia V, Jahangir A, Tajik J. Giant colloid cyst of the brain masquerading as vasovagal syncope. Heart Rhythm Case Reports. 2019; 5: 314–316.
5. Ebel F, Greuter L, Guzman R, Soleman J. Resection of brain lesions with a neuroendoscopic ultrasonic aspirator – a systematic literature review. Neurosurgical Review. 2022; 45: 3109–3118.
6. Singh H, Burhan Janjua M, Ahmed M, Esquenazi Y, et al. Factors influencing outcome in patients with colloid cysts who present with acute neurological deterioration. J Clin Neurosci. 2018; 54: 88–95.
7. Kabashi A, Dedushi K, Ymeri L, et al. Colloid cyst of the third ventricle: Case report and literature review. Acta Inform Med. 2020 Dec; 28(4): 283–286.
8. Roberts A, Jackson A, Bangar S, et al. Colloid cyst of the third ventricle. J Am Coll Emerg Physicians Open. 2021; 2(4): e12503.
9. Stokum JA, Gerzanich V, Simard JM. Molecular pathophysiology of cerebral edema. J Cereb Blood Flow Metab. 2016; 36(3): 513–538.
10. Visish M, Srinavasan MD, O'Neill BR, et al. The history of external ventricular drainage. Historical vignette. J Neurosurg. 2013; 120(1): 228–236.
11. Gerstl JVE, Aquilina K, Florman JE. Rare large colloid cyst obstructing the posterior third ventricle: illustrative case. J Neurosurg. 2021 Apr 12; 1(15): CASE2121.
12. Melicher D, Gaál S, Berényi T, et al. Acute hydrocephalus caused by a colloid cyst – a case report. Int J Emerg Med. 2023 Apr 19; 16(1): 28.
13. Stokum JA, Gerzanich V, Simard JM. Molecular pathophysiology of cerebral edema. J Cereb Blood Flow Metab. 2016 Mar; 36(3): 513–38.

Imaging Findings of Solitary Fibrous Tumors of the Gallbladder

Trinh Anh Tuan[1,2], Le-Thi Mai Huong[2], Nguyen Thu Minh Chau[2], Ngo Quang Duy[2,3], Nguyen-Thi Hai Anh[4], Nguyen Duy Hung[1,2], Luc Ceugnart[5], Nguyen Minh Duc[6,*]

ABSTRACT
Solitary Fibrous Tumor (SFT) is a rare mesenchymal tumor with a higher incidence of benign than malignant, most common location in the pleura. Although this tumor has been found in other locations in the body such as the head and neck region, retroperitoneal space, and intra-abdominal omentum, SFT of the gallbladder remains extremely rare in the medical literature. In this article, we present the imaging characteristics of Computed Tomography (CT) and Magnetic Resonance Imaging (MRI) of gallbladder SFT, thereby contributing to providing information in the study of this rare pathology.

KEYWORDS
solitary fibrous tumor; computed tomography; magnetic resonance imaging

AUTHOR AFFILIATIONS
[1] Department of Radiology, Viet Duc Hospital, Hanoi, Vietnam
[2] Department of Radiology, Hanoi Medical University, Hanoi, Vietnam
[3] Department of Radiology, Ha Giang General Hospital, Ha Giang, Vietnam
[4] Department of Radiology, Alexandra Lepève Hospital, Dunkirk, France
[5] Department of Radiology, Centre Oscar Lambret, Lille, France
[6] Department of Radiology, Pham Ngoc Thach University of Medicine, Ho Chi Minh City, Vietnam
* Corresponding author: Department of Radiology, Pham Ngoc Thach University of Medicine, Ho Chi Minh City, Vietnam; bsnguyenminhduc@pnt.edu.vn

Received: 28 October 2024
Accepted: 4 December 2024
Published online: 18 February 2025

Acta Medica (Hradec Králové) 2024; 67(3): 96–100
https://doi.org/10.14712/18059694.2025.5

INTRODUCTION

Solitary Fibrous Tumor (SFT) is an uncommon mesenchymal tumor, formerly also known as Hemangiopericytoma, that develops mainly in the pleura, belonging to the group of fibroblastic neoplasms with intermediate behavior according to the World Health Organization (WHO) classification of bone and soft tissue tumors (1, 2). Although less common than the pleura, SFTs in other locations such as the thyroid, greater omentum, retroperitoneum, or pelvis have occasionally been recorded (3). On the other hand, the Solitary Fibrous Tumor of the Gallbladder (SFTG) is nearly unique in the medical literature. According to our knowledge, there are only two cases of SFTG reported in the literature and one case was reported as hemangiopericytoma which is the previous terminology of SFTG in 1983 (2, 4, 5). This neoplasm is typically insidious in clinical symptoms and imaging characteristics, which easily overlaps with other entities. Hence, definitive diagnoses in the majority of cases rely heavily on biopsy results[2]. In this article, the imaging features of SFTG on Computed Tomography (CT) and Magnetic Resonance Imaging (MRI) are described with literature review.

CASE REPORT

A 41-year-old male patient with no medical history accidentally detected a mass in the right hypochondriac region three months before admission. He denied any pain, weight loss, or other clinical symptoms. A clinical examination of the abdomen revealed a hard and mobile area in the right hypochondrum. Further assessment of a Computer tomography (CT) scan on the chest and abdomen with contrast injection further detected a mass measuring 71 × 57mm with a uniform density before injection, lying at the level of the bottom of the gallbladder (arrow, Figure 1A) and extending downwards (star sign, Figurer 1A). The post-contrast image demonstrated the mass continuous with the base wall of the gallbladder (arrow mark, Figure 1B), extending downward with clear boundaries with surrounding structures (star mark, Figure 1B), and abundant vascular supply inside the mass (arrow Figure 1C). There were no other organ abnormalities on a chest and abdomen CT scan suggesting secondary lesions. Blood tests showed an increased white blood cell count of 16.28 G/L and normal red blood cell, as well as platelet counts with indexes of 4.62 T/L and 260 G/L, respectively. Blood biochemical tests showed normal total and direct bilirubin with indexes of 7umol/l and 2umol/l, respectively, and a normal GGT index of 32 U/I. On the hepatobiliary MRI, the T2-weighted (T2W) sequence showed a heterogeneous hypointense mass (Figure 2A arrow) with a well-defined border. The post-contrast image demonstrated heterogenously strong enhancement in the arterial phase (arrow, Figure 2B) and more contrast loading on the venous phase (arrow, Figure 2C). The mass located next to the D2 duodenum region. It showed no signs of invasion or compression of the extrahepatic bile ducts or liver parenchyma. There were no abnormal lymph nodes in the abdomen.

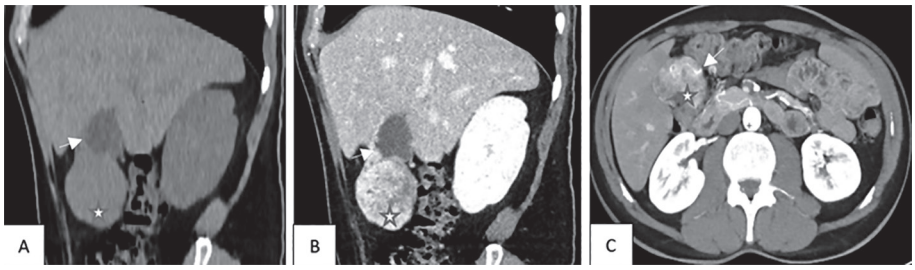

Fig 1 Image A Sagittal plane before contrast injection, tumor located at the base of the gallbladder (arrow) with relatively clear boundaries, uniform density, growing downwards (star sign). Image B Sagittal plane, portal vein phase, clearly observed tumor continuous with gallbladder base wall (arrow), strong and heterogenous enhancement (star sign). Image C Axial plane shows strong and irregular enhancement of the tumor artery (star sign); branch vessels are inside the tumor, which can be seen more clearly using the MIP reconstruction. (Maximum Intensity Projection).

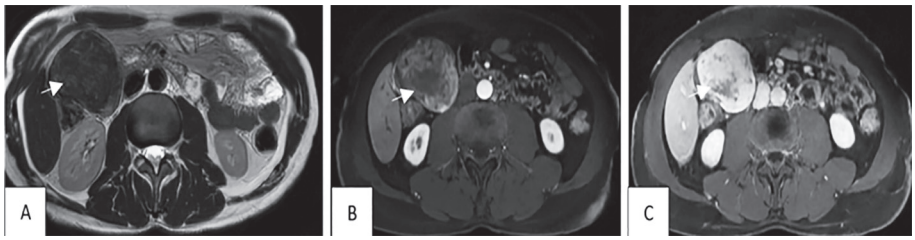

Fig 2 Image A Axial T2W sequence, the tumor has clear boundaries and a heterogeneous signal, with some hypointensity suggesting collagenous or fibrous stroma (arrow). Image B Axial T1FS arterial phase sequence, tumor enhances strongly but heterogeneously (arrow). In the image C Axial T1FS sequence in the venous phase, the tumor enhances strongly and more than in the arterial phase (arrow).

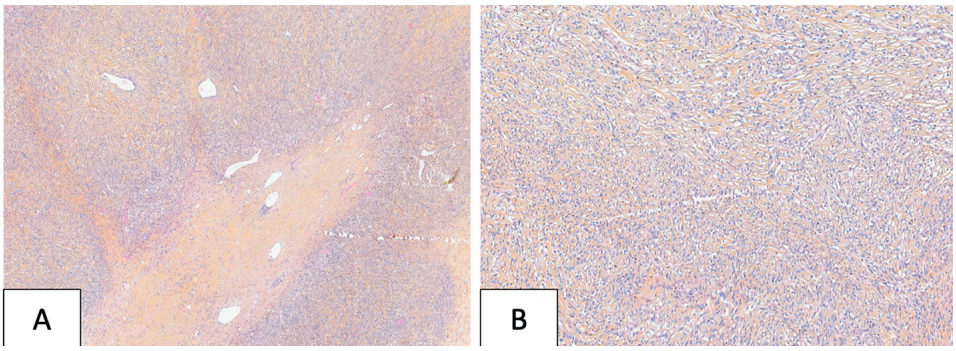

Fig 3 HPS staining. (A) HPS x250: alternation of cellular and hypocellular zone, hemangiopericytic vascularization. (B) HPS x100: monomorphic spindle cells, not atypical, low mitotic index. HPS = Hémalun, Phloxine, Safran.

After multidisciplinary consultation, the patient was treated with laparoscopic surgery to remove the gallbladder and tumor into a single mass. On postoperative pathology, microscopic tumor cell density ranged from moderate to high. Tumor cells are spindle-shaped, round-nucleated, and monomorphic, arranged in short bundles on a collagen-rich stromal base. Blood vessels behave as the hemangiopericytic type. There are areas of fibrosis, hyalinization, and poor cells. There are two divisions on ten fields with X400 magnification (field diameter is 0.62 mm). Immunohistochemical staining of anti-STAT6 antibody was strongly positive for nuclei of tumor cells. The histopathological results of the tumor concluded that it was an SFTG with a low risk of metastasis, according to Demicco risk stratification systems. The patient was stable after surgery and was discharged with regular follow-up examination.

DISCUSSION

SFT is a histologically characterized mesenchymal neoplasm originating from fibroblastic or myofibroblastic cells. It usually arises in the pleural cavity, with the first recognized case being described by Klemperer and Rabin in 1931. Until now, approximately 30–40% of SFT cases outside the pleural membrane have been reported in the medical documents (6–8). Although SFT can be found in multiple locations throughout the body, SFT in the abdominal cavity, and especially SFTG, is exceptionally rarely mentioned in medical texts. It is worth mentioning that the WHO has recently standardized the general terminology for SFT and Hemangiopericytoma using the term SFT (1–3). In general, SFT is considered a benign tumor with a rate of approximately 78–88% of cases. It typically does not significantly affect the patient's prognosis. However, there is still a rate of roughly 12–22% of SFT cases that progress into a malignant form, which can invade and metastasize. The recurrence rate of SFT is 6%, according to Decouvelaere et al. (7). Due to the malignant potential of SFT, mainly when the tumor size is > 10 cm, early diagnosis of SFT is crucial to excise the tumor and prevent its cancerous possibility. However, it still takes a huge of effort to give a definitive diagnosis of SFT preoperatively (7).

Clinically, SFT tumors outside the lung membrane commonly occur in middle-aged individuals, with an equal prevalence between males and females. They typically present a silent and asymptomatic development. However, when the tumor grows, it may manifest symptoms due to compression of nearby structures. Furthermore, less than 5% of SFT patients exhibit signs of hypoglycemia (6). Some clinical features that may occur in abdominal SFT include abdominal pain, palpable mass, and gastrointestinal or urinary symptoms due to the mass effect of the tumor (6). Two reported cases of benign include a 55-year-old female patient incidentally discovered during follow-up for breast fibroadenoma and an 83-year-old female patient admitted to the hospital due to recurrent upper abdominal pain for several months. On the other hand, the malignant case of Hemangiopericytoma of the gallbladder involved a 30-year-old female patient who was hospitalized for the development of a right upper quadrant abdominal mass over five months (2, 4, 5). In our report, a 41-year-old male patient was admitted to the hospital due to self-palpation of a painless mass located on the right lower chest wall, with no other accompanying symptoms. As a result, imaging diagnostic examinations are necessary to define the specific characteristics of SFT in general and SFTG in particular.

On ultrasound, typical SFT tumors often appear hypoechoic but occasionally with heterogeneous echoic structures corresponding to areas of myxoid degeneration within the lesion. Furthermore, despite SFT being a highly vascular tumor, color Doppler ultrasound typically does not demonstrate flow signals (8). On CT, SFT tumors frequently exhibit well-defined borders and heterogeneous density. They may occasionally demonstrate calcification, although it is rare. After contrast administration, the tumor displays highly vascular, but the central region may show decreased density, indicating necrosis or cystic degeneration within the tumor (6). In addition, determining the correlation of the tumor with adjacent structures, including signs of compression or invasion, and searching for any potential metastatic lesions, if present, is an advantage of CT in diagnosing and planning the treatment for patients. MRI with high soft tissue resolution, multiple sequences, and imaging planes defines the composition and nature of SFT better than CT and ultrasound. Nevertheless,

the features of SFT tumors on MRI can differ based on the amount of collagenous or fibrous stroma, vascularity, and cell density. On T1W images, the tumor typically exhibits intermediate signal intensity, while on T2W, the tumor shows heterogeneous low signal intensity corresponding to the collagenous or fibrous stroma component (Figure 2A). Image B T1FS Axial arterial phase pulse sequence, tumor enhances strongly but heterogeneously (arrow). Image C Axial T1FS pulse sequence in the venous phase, the tumor enhances strongly and more when compared to the arterial phase (arrow). After gadolinium injection, the tumor demonstrates strong and heterogeneous enhancement, with possible areas of non-enhancement in the core region. Additionally, the presence of tortuous blood vessels at the edge of the tumor is a visible indicator that can help confirm the diagnosis (Figure 1C) (6). Moreover, the dynamics of contrast enhancement in SFT tumors are also remarkable, exhibiting mild arterial phase enhancement, increased venous phase enhancement, and late enhancement, suggesting the existence of fibrous or collagenous stroma inside the tumor (Figure 2C) (6). Angiography is also worthy of vascular-rich neoplasms like SFT, with images showing increased vascularity and a feeding artery supplying the tumor. Dilated arterial branches within the tumor as well as the early visualization of veins (arteriovenous shunt) can also be observed (6).

Because SFTG is an uncommon lesion, it might be challenging to differentiate it from other gallbladder tumors clinically and imaging. This fact explains the unusual appearance of SFTG in the medical literature. Based on the anatomical location of the tumor in the gallbladder fundus, we identified two differential diagnoses that need to be considered in this case, including Gallbladder adenomyomatosis and Gallbladder Carcinoma. Gallbladder Adenomyomatosis is a benign lesion characterized by hypertrophy of the mucosal layer with invasion into the muscular layer, forming Rokitansky-Aschoff sinuses. It is manifested on ultrasound by comet-tail artifacts when cholesterol crystals are deposited inside. In addition, on MRI, the feature "pearl necklace sign" is notable in Gallbladder Adenomyomatosis, with increased signal intensity on T2W images, resembling the pearls on a necklace (9). On the other hand, contrast enhancement following injection is usually uneven in malignant tumors such as gallbladder carcinoma, showing an invading tendency to surrounding structures, especially the liver parenchyma, as well as the presence of metastatic lymph nodes (10).

Histopathological features are the gold standard for diagnosing SFT and distinguishing it from other types of tumors. On a histological level, SFT tumors typically grow from spindle cells and submesothelial stromal cells with a fibroblastic or myofibroblastic phenotype. However, the diagnosis can overlap with other conditions, such as mesothelioma and leiomyoma (11). The diagnosis is confirmed by immunohistochemistry, which shows that SFT tumor cells test negative for cytokeratins, S-100, and Desmin but positive for CD34, CD99, and BCL-2 (3, 11). It is important to mention that histopathological features and the Ki67 index are helpful in diagnosing malignant SFT (12).

Surgery is the primary treatment for SFT in general and SFTG in particular. Its goal is to reduce the tumor's chance of becoming malignant. Some factors positively associated with the malignancy potential of the tumor include a size greater than 10 cm and a high mitosis rate (> 4 per 10 high-power fields or > 4 mitoses per 2 mm^2) (11). Due to the SFT tumor's high vascular characteristic, performing preoperative embolization is encouraged to reduce the risk of bleeding during surgery (6). Up until now, there is no clear evidence of the benefits of treating SFT with radiotherapy or systemic therapies. However, systemic treatment should be considered for malignant cases with recurrent or metastatic lesions, even though at a low rate (11). Post-operative monitoring after surgical removal of SFT tumors is necessary, especially for malignant SFT tumors, due to the rate of local recurrence and metastasis (3). On surveillance of 81 SFT patients, author Winan found that the 5-year survival rate was 84%, with local recurrence and metastasis rates of 29% and 34%, respectively (11).

CONCLUSION

A solitary Fibrous Tumor is a mesenchymal tumor that is usually benign, while occasional malignant cases have been reported, mainly in the pleural membrane rather than other places. SFTs in the gallbladder are extremely rare. Early diagnosis and early surgical treatment are necessary to prevent the potential malignant progression of the tumor over time, thereby improving treatment effectiveness. Although the occurrence in the gall bladder is uncommon, SFT should be considered in some instances, especially when there are suggestive diagnostic features in imaging studies. On CT and MRI, some critical signs that indicate the diagnosis of SFT include well-defined borders, high-vascularity, and decreased signal on T2W imaging with more contrast enhancement in the arterial and late phases, suggesting the presence of fibrous or collagenous stroma within the tumor. In addition, the presence of tortuous dilated blood vessels in the periphery of the tumor is also a feature that helps confirm the diagnosis.

AVAILABILITY OF DATA AND MATERIALS

Data and materials used and/or analyzed during the current study are available from the corresponding author on reasonable request.

ETHICS APPROVAL AND CONSENT TO PARTICIPATE

Our institution does not require ethical approval for reporting individual cases or case series. Written informed consent was obtained from the patient(s) for their anonymized information to be published in this article.

REFERENCES

1. Fletcher CDM. The evolving classification of soft tissue tumours – an update based on the new 2013 WHO classification. Histopathology. 2014; 64(1): 2–11.
2. Almasri M, Aljalabneh B, Mureb A, Khzouz J. Solitary fibrous tumour of the gallbladder: A rare case report. Int J Surg Case Rep. 2023; 106: 108256.

3. Rodriguez Tarrega E, Hidalgo Mora JJ, Paya Amate V, Vega Oomen O. Solitary fibrous tumor of the greater omentum mimicking an ovarian tumor in a young woman. Gynecol Oncol Rep. 2016; 17: 16–19.
4. Gupta S, Padmanabhan A, Khanna S. Malignant hemangiopericytoma of the gallbladder. J Surg Oncol. 1983; 22(3): 171–174.
5. Lazure T, Dimet S, Ndiaye N, Bourdin G, Ladouch-Badre A. Giant cell-rich solitary fibrous tumour of the gallbladder. First case report. Histopathology. 2007; 50(6): 805–807.
6. Shanbhogue AK, Prasad SR, Takahashi N, Vikram R, Zaheer A, Sandrasegaran K. Somatic and Visceral Solitary Fibrous Tumors in the Abdomen and Pelvis: Cross-sectional Imaging Spectrum. Radiographics. 2011; 31(2): 393–408.
7. Urabe M, Yamagata Y, Aikou S, et al. Solitary Fibrous Tumor of the Greater Omentum, Mimicking Gastrointestinal Stromal Tumor of the Small Intestine: A Case Report. Int Surg. 2015; 100(5): 836–840.
8. Ginat DT, Bokhari A, Bhatt S, Dogra V. Imaging Features of Solitary Fibrous Tumors. AJR Am J Roentgenol. 2011; 196(3): 487–495.
9. Golse N, Lewin M, Rode A, Sebagh M, Mabrut JY. Gallbladder adenomyomatosis: Diagnosis and management. J Visc Surg. 2017; 154(5): 345–353.
10. Lopes Vendrami C, Magnetta MJ, Mittal PK, Moreno CC, Miller FH. Gallbladder Carcinoma and Its Differential Diagnosis at MRI: What Radiologists Should Know. Radiographics. 2021; 41(1): 78–95.
11. Van Houdt WJ, Westerveld CMA, Vrijenhoek JEP, et al. Prognosis of Solitary Fibrous Tumors: A Multicenter Study. Ann Surg Oncol. 2013; 20(13): 4090–4095.
12. Ambardjieva M, Saidi S, Jovanovic R, et al. Solitary Fibrous Tumor of Adrenal Gland and Review of the Literature. Pril (Makedon Akad Nauk Umet Odd Med Nauki). 2021; 42(3): 63–69.